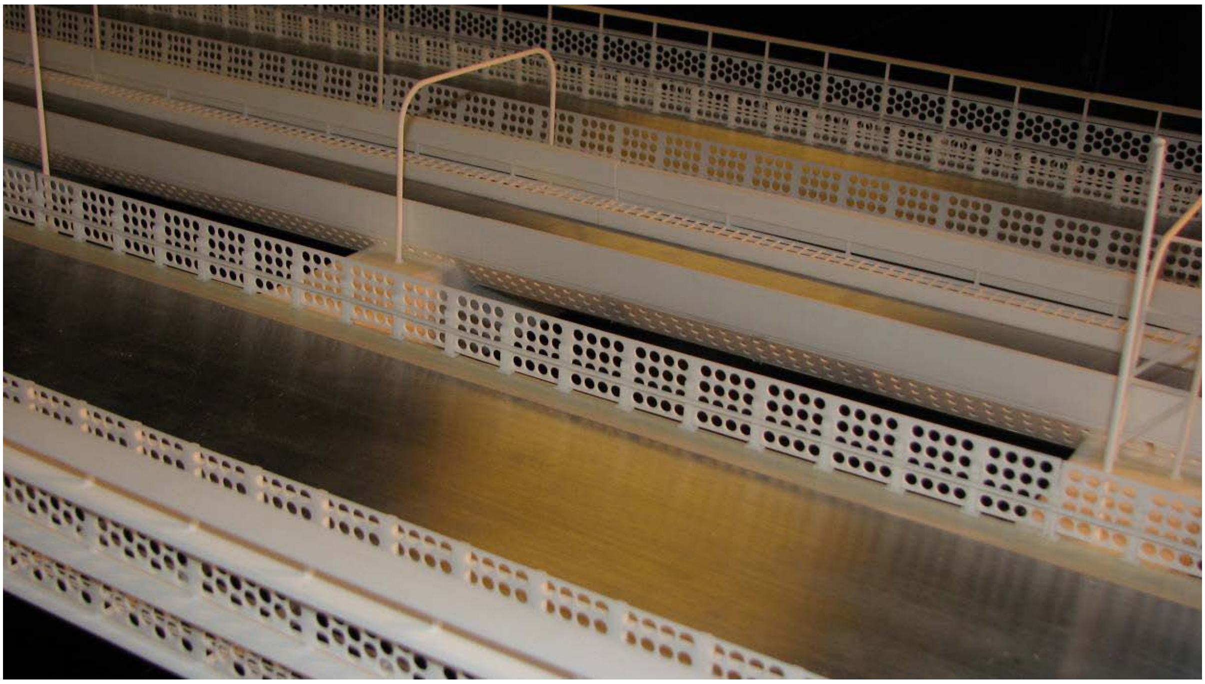

EUROLINK S.c.p.A

Indicative Vortex-Shedding Tests,

Static & Stability Tests for the Messina Strait Bridge

FORCE 110-26444.02 Rev. 1/2010-12-07

Project No. and Title of Report:

FORCE 110-26444.02
Indicative Vortex-Shedding Tests, Static & Stability Tests
for the Messina Strait Bridge

Client: EUROLINK S.c.p.A	**Client's Ref.:** Allan Larsen, COWI A/S
Author(s): Søren V. Larsen	**Date:** 2010-12-07
	Approved by:

Revision	Description	By	Checked	Approved	Date
1	Final report (no comments received)	SVL	AD	AD	7/12 2010
B	Table 8.2 corrected (PDF version)	SVL	SGe	SS	2010-08-30
A	Issued for Client's Comments (PDF version)	SVL	AaD	CRS	2010-08-26

Keywords:
Suspension Bridge.
Section Model Tests.
Vortex-Shedding.

Classification:
- ☐ Open
- ☐ Internal
- ■ Confidential

GTS ADVANCED TECHNOLOGY GROUP

FORCE Technology, Kgs. Lyngby
Hjortekærsvej 99
2800 Kgs. Lyngby, Denmark
Tel. +45 72 15 77 00
Fax +45 72 15 77 01

FORCE Technology Norway AS
Claude Monets allé 5
1338 Sandvika, Norway
Tel. +47 64 00 35 00
Fax +47 64 00 35 01
info@forcetechnology.no
www.forcetechnology.no

FORCE Technology Sweden AB
Tallmätargatan 7
721 34 Västerås, Sweden
Tel. +46 (0)21 490 3000
Fax +46 (0)21 490 3001
info@forcetechnology.se
www.forcetechnology.se

FORCE Technology,Headquaters
Park Allé 345
2605 Brøndby, Denmark
Tel. +45 43 26 70 00
Fax +45 43 26 70 11
force@force.dk
www.forcetechnology.dk

LIST OF CONTENTS:

APPENDICES:

1. Introduction

FORCE Technology was commissioned by EUROLINK S.c.p.A to conduct an indicative investigation of vortex-induced oscillations of the bridge deck of the Messina Strait Bridge. Further, static tests, and stability and damping tests were conducted. COWI A/S acted as the Client's representative. The present section model tests were conducted as extension to the test programme identified as Sub-test D4.

The present report describes the indicative section model tests performed to investigate the vortex-induced oscillations for the bridge deck for a number of configurations of the road and railway girders. Furthermore, static force coefficients were determined for some of the configurations. Finally, the stability limits were determined as well as the damping levels at two wind speeds.

The section model tests were performed on a 1:80-scale section model of the bridge deck in FORCE Technology's 2.6 m wide boundary-layer wind tunnel. The tests were conducted at FORCE Technology in August 2010.

The work was performed as an extension to the Agreement between FORCE Technology and Eurolink S.c.p.A. dated 2010-06-21. The present work was performed according to Addendum 1 (dated 2010-08-03) and according to parts of Addendum 2 (dated 2010-11-04), respectively.

2. Summary and Conclusions

This report presents the results of the wind-tunnel tests conducted to establish aerodynamic data for various configurations of the bridge girder for the Messina Strait Bridge.

A 2.55 m long section model built at a geometric scale of 1:80 for previous investigations was used and modified for the present tests. The model was tested in smooth flow and turbulent flow in FORCE Technology's 2.6 m wide Boundary-Layer Wind Tunnel.

The following aerodynamic parameters were established:

1) Indicative vortex-shedding response in smooth flow for 10 configurations
2) Static force coefficients in smooth flow for 4 configurations
3) Aerodynamic stability and damping in smooth and turbulent flow for 2 configurations

All tests in this series were conducted with the road girders having 2% outward slope.

The main findings are summarised in the following. The various configurations are described in Section 3.1.

Indicative Vortex-Shedding Tests

The deck section's susceptibility to vortex-shedding induced oscillations was investigated for a number of geometric configurations in the static rig. These indicative tests were conducted in smooth flow and at an angle of wind incidence of 0°.

Up to two vortex-shedding induced vertical response peaks were identified for each configuration. The first peak was found at reduced velocities on the range $0.4<U_{red}<0.55$, where $U_{red}= U/(f_v \cdot B)$ (f_v = vertical frequency and B = deck width). The second peak was found in the range $0.6<U_{red}<0.9$. The table below summarises the root-mean-square (rms) vertical displacement at mid span of the model. The rms displacements were estimated by double-integration of the acceleration measured at the mid span of the model.

#	Configuration	Rms vertical disp. / H 1st peak [% of H]	Rms vertical disp. / H 2nd peak [% of H]
1	C5	2.5	1.5
2	C2	0.5	2.4
3	C7	0.6	1.0
4	C8	2.1	3.4
5	C5 with sharp road girder edge	2.3	1.7
6	C7 with sharp road girder edge	0.4	1.1
7	C2 with 45° rail girder edge	0.7	(0.1)
8	C2 with 80° rail girder edge	0.8	-
9	C5 with 45° rail girder edge	2.5	(0.1)
10	C5 with 80° rail girder edge	2.3	-

Table 2.1. Summary of normalized vertical rms displacements in indicative vortex-shedding tests.

Static Tests

The static force coefficients at 0° and their variations with angle of wind incidence (first derivatives) are shown in Table 2.2. Figure 6.2 and Figure 6.3 show plots of all the determined coefficients for the various configurations, with the drag and lift coefficients, C_d and C_l, being fixed in a wind coordinate system, and C_x and C_z being body fixed coefficients, see Section 6.

		C2 45° rail girder edge	C2 80° rail girder edge	C5 45° rail girder edge	C5 80° rail girder edge
C_d	(0°)	0.104	0.106	0.104	0.103
C_l	(0°)	-0.040	-0.046	-0.061	-0.063
C_m	(0°)	0.008	0.007	0.004	0.004
$\frac{dC_d}{d\alpha}$	(-1° to +1°)	-0.03	-0.09	-0.05	-0.06
$\frac{dC_l}{d\alpha}$	(-1° to +1°)	0.06	-0.11	0.48	0.42
$\frac{dC_m}{d\alpha}$	(-1° to +1°)	0.15	0.13	0.21	0.21

Table 2.2. Static aerodynamic force coefficients and their slopes (based on a deck width of B= 60.4 m).

Stability Tests

The aerodynamic stability was investigated for the configuration C2 with 45° panels on the railway girder. Stability tests were conducted for ±4° and 0°, and in smooth and turbulent flow. Also C5 with 45° panels on the railway girders was tested for +4° in smooth flow.

The estimated critical wind speeds for onset of aerodynamic instability are listed in the following table.

Configuration	Flow	Angle	$U_{red,cr}$ $[U_{cr}/(f_t \cdot B)]$	U_{cr} [m/s]
C2 with 45° rail girder edge	Smooth	-4°	>25.2	>126
		0°	18.1	91
		+4	17.1*	86*
C2 with 45° rail girder edge	Turbulent	-4°	18.0	90
		0°	16.7	84
		+4°	17.6	88
C5 with 45° rail girder edge	Smooth	+4°	23.1	116

Table 2.3. Estimated aerodynamic stability limits as reduced wind speed $[U_{cr}/(f_t \cdot B)]$ and full-scale wind speed [m/s].

*For the configuration C2 / 45° in smooth flow at +4°, a limit-cycle response (i.e., large response self-limited in amplitude) was observed for this configuration and angle of attack for wind speeds lower than the estimated critical wind speed. The limit-cycle responses were dominated by vertical motion and with a moderate torsional response, the latter with a frequency coinciding with the vertical frequency.

Aerodynamic Damping

In connection with the stability tests the damping of the bridge section was estimated based on free decay tests conducted at wind speeds corresponding to 54 m/s and 75 m/s full-scale, respectively. Results are presented in Section 8.2. Damping tests were conducted for configuration C2, only.

3. Model Design

3.1 Prototype Structure

The Messina Strait Crossing comprises a suspended main span of 3300 m. The total length of the bridge is 3666 m. The bridge deck comprises three closed box girders and the overall deck width is approximately 60 m.

An elevation of the prototype structure is shown in Figure 3.1.

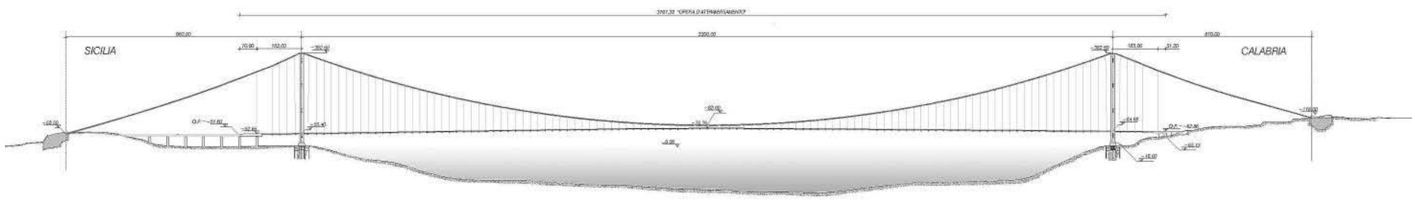

Figure 3.1 Elevation of the Messina Strait Crossing.

Figure 3.1 shows the cross section of the prototype bridge deck and its main dimensions.

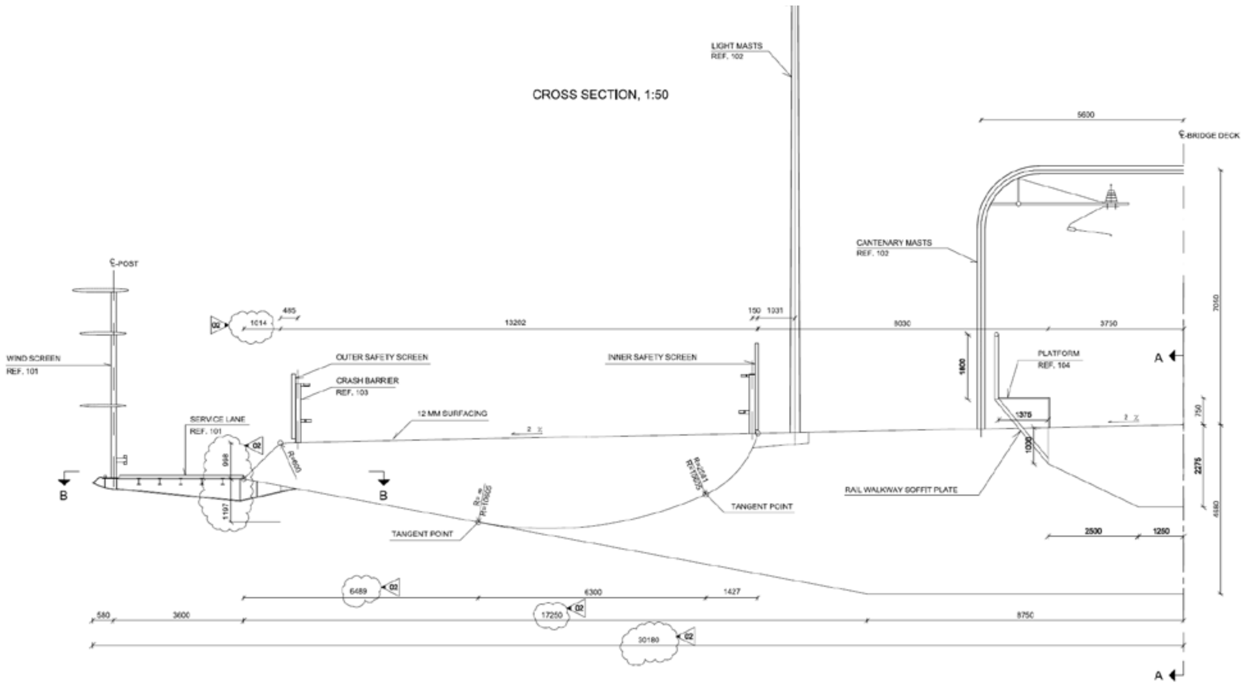

Figure 3.2. Cross-section of prototype bridge deck.

3.2 Scaling Parameters

A combination of geometrical, mass and stiffness considerations resulted in the selection of a 1:80 geometrical scale for the section model of the Messina Strait Bridge deck, see [1].

For the present tests, the model designed and constructed for the Sub-tests D4 was used.

3.3 Section Model Design

The 1:80 geometrical scale section model of the bridge deck was built with the properly scaled outer shape of the prototype structure. The various configurations were obtained by using the different screens from the Sub-tests 1, see [4]. Other configurations were obtained by mounting edge fairings produced by model foam onto the model. These edge fairings were produced according to drawings/sketches supplied by the Client's representative.

The tested configurations and their details are described in the following. For completeness all configurations from Sub-Test 1 are listed in the table below together with a new configuration referred to as C8 (inner safety screens only). It should be noted that configuration C8 was not included in the previous tests (110-25465), but in the present test programme only.

#	Inner Safety Screens (2.4m)	Outer Safety Screens (1.8m)	Soffit Plate	Solid Railway Screen
C1	off	off	off	on
C2	**off**	**off**	**porous**	**on**
C3	off	off	solid	on
C4	on	off	porous	on
C5	**on**	**on**	**porous**	**on**
C6	on	off	porous	off
C7	off	off	porous	off
C8	**on**	**off**	**porous**	**off**

Table 3.1. Summary of screen configuration.

The positions of the screens are shown in the following figure.

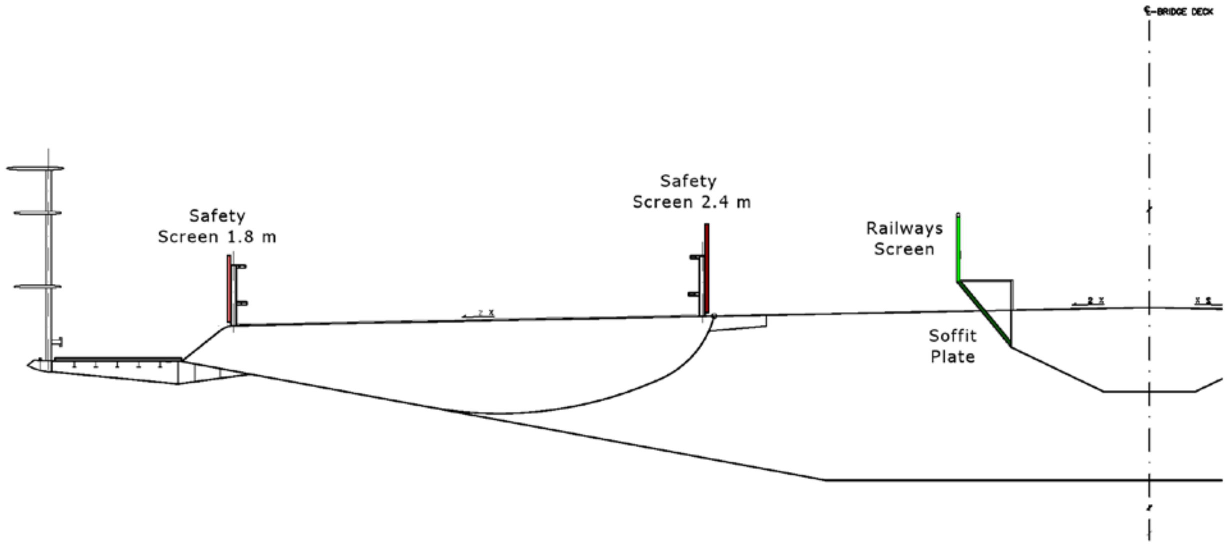

Figure 3.3. Positions of screens on the bridge deck.

Configurations C5 and C7 were tested with a sharp edge configuration of the inner lower panel on the road deck girder, as illustrated in the figure below. This is referred to as *sharp road girder edge*.

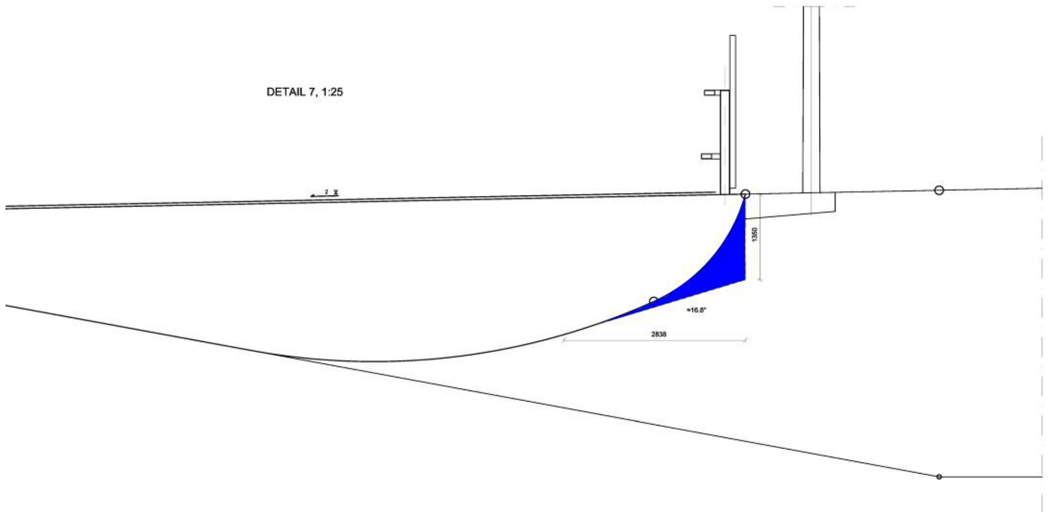

Figure 3.4. Sharp edge configuration – sharp road deck girder edge.

Figure 3.5. Photograph of sharp edge configuration – road deck girder.

Configurations C2 and C5 were tested with modified lower panels on the railway girder, as illustrated in the following figures. These two configurations are referred to as *45° rail girder edge* and *80° rail girder edge,* respectively. Both these configuration had the rounded edge on the road girder.

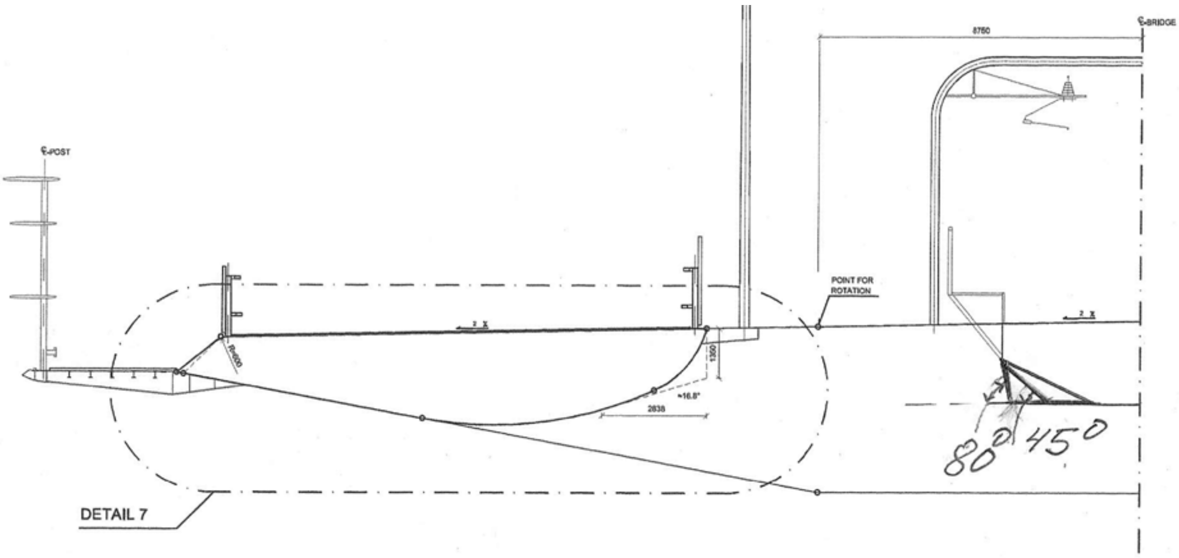

Figure 3.6. Modified railway girder configurations – 45° and 80° rail girder edge.

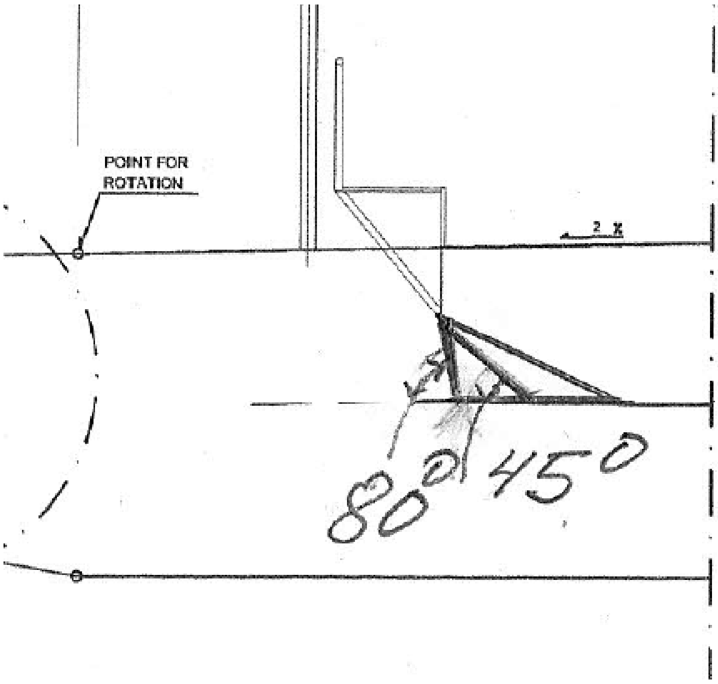

Figure 3.7. Modified railway girder configurations – 45° and 80° rail girder edge (detail).

Figure 3.8. Photographs of 45° rail girder edge.

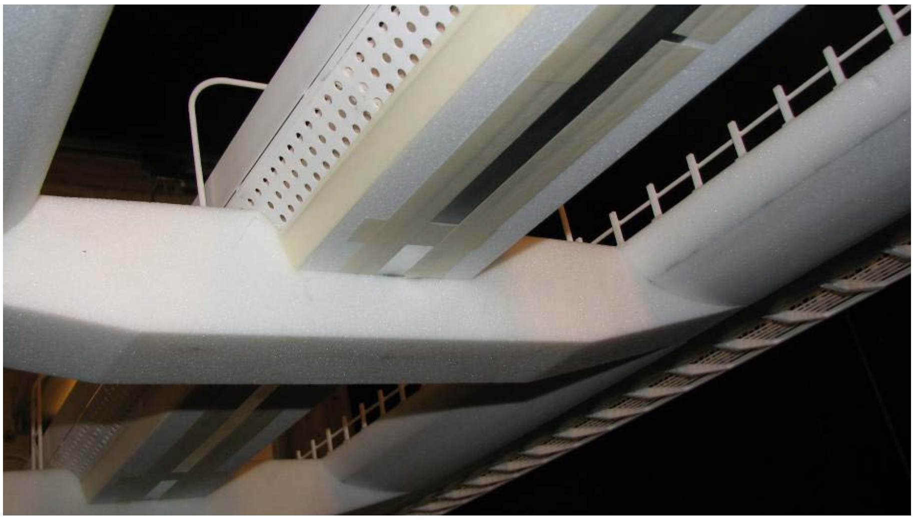

Figure 3.9. Photographs of 80° rail girder edge.

4. Wind Tunnel and Flow Conditions

The section model tests were conducted in FORCE Technology's 2.6 m wide x 1.8 m high x 21 m long Boundary-Layer Wind Tunnel II. The model was placed 14.5 m downstream of the inlet at the mid height of the wind tunnel. The ceiling of the wind tunnel was adjusted so that it was horizontal throughout the length of the wind tunnel.

The wind-tunnel tests were performed in smooth and turbulent flow. The smooth flow condition corresponds to an empty tunnel (i.e., without exposure upwind of the model). The smooth flow condition has a turbulence intensity ($I_{u,w}$) of approximately 0.5%.

The turbulent exposure was obtained by three spires mounted 1.1 m from the wind tunnel inlet. The spires were 1.8 m high with a tapered width: 0.32 m at the floor to 0.18 m at the wind tunnel ceiling. This exposure resulted in turbulence intensities of approximately 7.5% for I_u and 7.4% for I_w.

5. Wind-Tunnel Test Programme

The test programme consisted of static and dynamic section model tests, the objective being to determine the static wind loads, vortex shedding characteristic and the aerodynamic stability.

The detailed test programme is outlined in Table 5.1.

#	Test	Angles	Configuration	Flow
1	Indicative vortex tests	0°	C5	Smooth
2	Indicative vortex tests	0°	C2	Smooth
3	Indicative vortex tests	0°	C7	Smooth
4	Indicative vortex tests	0°	C8	Smooth
5	Indicative vortex tests	0°	C5 sharp road girder edge	Smooth
6	Indicative vortex tests	0°	C7 sharp road girder edge	Smooth
7	Indicative vortex tests	0°	C2 45° rail girder edge	Smooth
8	Indicative vortex tests	0°	C2 80° rail girder edge	Smooth
9	Indicative vortex tests	0°	C5 45° rail girder edge	Smooth
10	Indicative vortex tests	0°	C5 80° rail girder edge	Smooth
11	Stability and damping tests	-4°, 0°, +4°	C2 45° rail girder edge	Smooth
11a	Stability tests	+4°	C5 45° rail girder edge	Smooth
12	Stability and damping tests	-4°, 0°, +4°	C2 45° rail girder edge	Turbulent
13	Static tests	-10° to +10°, Δ=1°	C2 45° rail girder edge	Smooth
14	Static tests	-10° to +10°, Δ=1°	C2 80° rail girder edge	Smooth
15	Static tests	-10° to +10°, Δ=1°	C5 45° rail girder edge	Smooth
16	Static tests	-10° to +10°, Δ=1°	C5 80° rail girder edge	Smooth

Table 5.1. Test programme for section model tests.

6. Static Tests

6.1 Static Force Coefficients Definition

The static aerodynamic force coefficients for the deck of the Messina Strait Bridge were determined based on wind-tunnel tests on a 1:80 geometrical scale model of a section of the deck in smooth flow.

A typical force coefficient is defined as follows:

$$C_{x,z,l,d} = \frac{\overline{F}_{x,z,l,d}}{\overline{q}\,BL} \qquad (6.1a)$$

$$C_m = \frac{\overline{M}}{\overline{q}\,B^2 L} \qquad (6.1b)$$

Where:

C	=	Aerodynamic coefficient
$\overline{F}$	=	Time-averaged (mean) aerodynamic force
$\overline{M}$	=	Mean overturning moment (torque)
B	=	The bridge deck width (60.4 m in the present case, 60.74 m for previous tests)
L	=	The model span length
$\overline{q}$	=	The mean wind velocity pressure[1] at deck level; $\overline{q} = \frac{1}{2}\rho\overline{V^2}$ where:
ρ	=	Air density [kg/m^3]
$\overline{V}$	=	Mean wind velocity at deck level in [m/s]

The subscripts x, z, l, d and m refer to the x and z body-force components, lift, drag and overturning moment, respectively.

The procedure for the determination of the static coefficients consists of mounting the 2.55 m long section model of the bridge in a static rig equipped with two 3-component force balances. The force balances measure the vertical, lateral and torsional reactions at the extremities of the model. The reactions are combined to obtain: $\overline{F}_l, \overline{F}_d$ and $\overline{M}$, respectively.

These quantities are subsequently normalized according to the equations above. This procedure is repeated for several angles of attack of the model (from –10° to +10° in increments of 1^o, measured from the horizontal plane).

[1] The mean velocity pressure is measured directly (by micro manometers), consequently the value of the air density and the mean wind velocity are not determined explicitly.

The rate of change (or slope) of the coefficients with angle of attack α in radians is evaluated from these tests in the vicinity of zero degrees (between –1° and +1°).

The drag and lift coefficients, C_d and C_l, are defined in the global coordinate system in relation to the wind. The body force coefficients, C_x and C_z, defined in the local coordinate system, are linked to the drag and lift coefficients by the following relationships:

$$C_x(\alpha) = C_d(\alpha)\cos\alpha - C_l(\alpha)\sin\alpha \tag{6.2a}$$

$$C_z(\alpha) = C_d(\alpha)\sin\alpha + C_l(\alpha)\cos\alpha \tag{6.2b}$$

A bridge deck width, B, of 60.4 m (full-scale) was used in the determination of the coefficients. The centre of measurement of the forces and moment was set at the shear centre of the section, 1.33 m (in full-scale) above the bottom of the bottom plate of the railway girder.

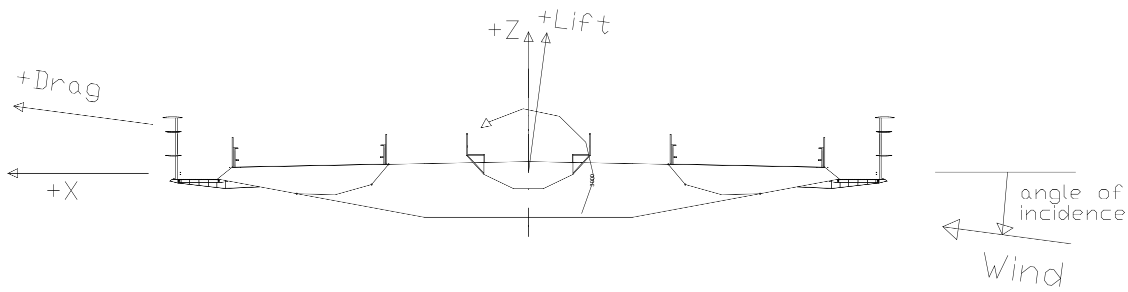

Figure 6.1. Sign convention for the static section model tests.

6.2 Results

The present tests were conducted at model-scale wind speeds of typically about 12 m/s. Figure 6.2 and Figure 6.3 present the variations of the coefficients with angle of wind incidence, α, for the bridge deck.

A summary of the main static coefficients is given in Table 2.2 of Section 2. The rate of change (slope) of the coefficients around 0° was calculated based on the values at –1° and +1°, see also the tables in Section 2.

The measured coefficients have been corrected for the effect of blockage according to ESDU[2]. The blockage correction was in the order of 3-7% depending on the deck inclination.

[2] Engineering Sciences Data Unit Item 80024:" Blockage correction for bluff bodies in confined flows", Nov. 1980.

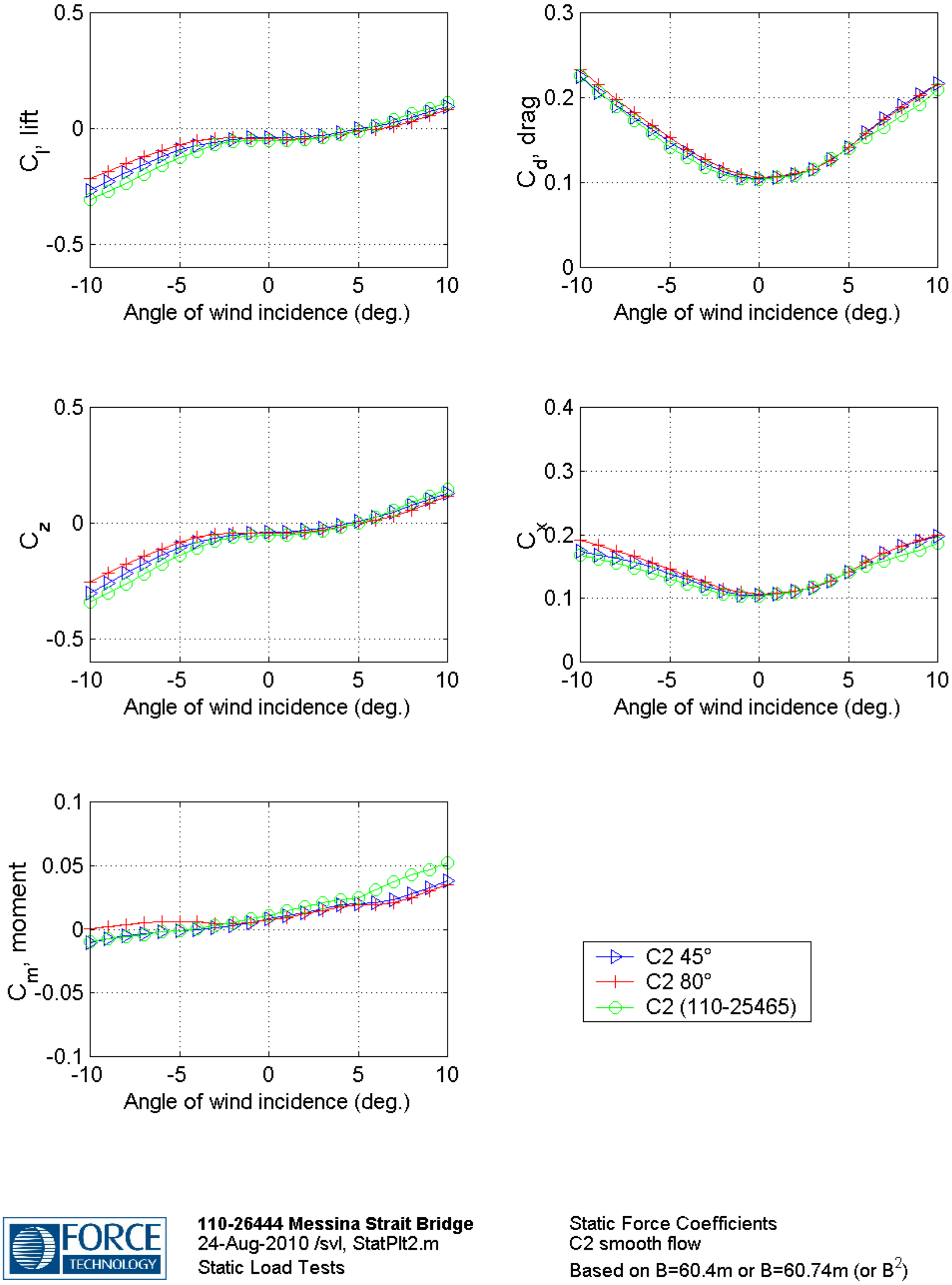

Figure 6.2. Variations of the static force coefficients – C2 configurations. Results based on deck width B. B=60.4 m in the present case, B=60.74 m for previous tests (110-25465).

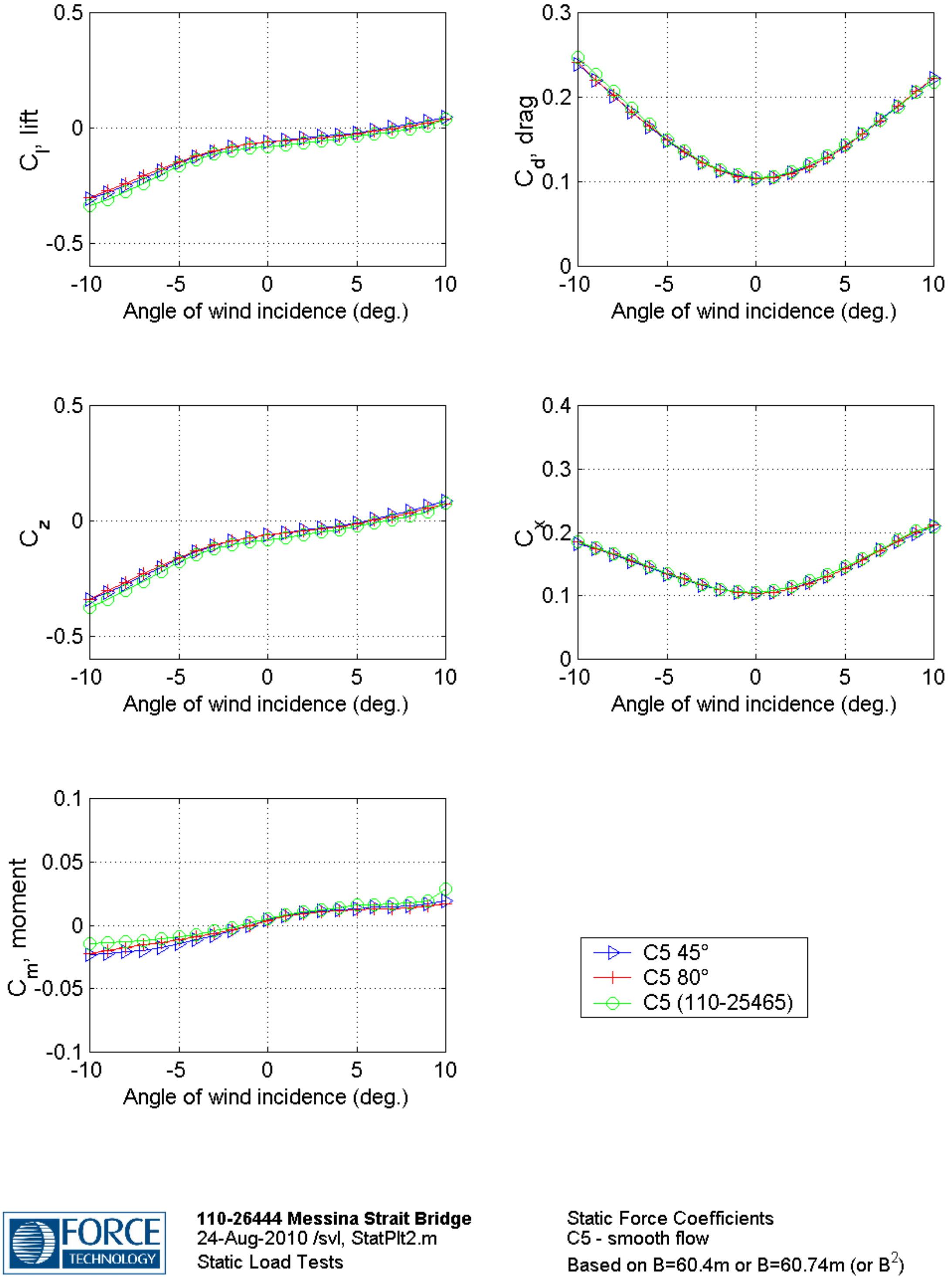

Figure 6.3. Variations of the static force coefficients – C5 configuration. Results based on deck width B. B=60.4 m in the present case, B=60.74 m for previous tests (110-25465).

	C2 45° rail girder edge			C2 80° rail girder edge			C5 45° rail girder edge			C5 80° rail girder edge		
α [°]	C_d	C_l	C_m	C_d	C_l	C_m	C_d	C_l	C_m	C_d	C_l	C_m
-10	0.224	-0.266	-0.010	0.232	-0.217	0.000	0.239	-0.306	-0.023	0.241	-0.304	-0.022
-9	0.206	-0.228	-0.007	0.215	-0.185	0.002	0.221	-0.280	-0.022	0.220	-0.270	-0.020
-8	0.191	-0.191	-0.005	0.198	-0.152	0.004	0.201	-0.250	-0.021	0.202	-0.240	-0.018
-7	0.176	-0.155	-0.004	0.182	-0.122	0.005	0.183	-0.219	-0.020	0.182	-0.207	-0.016
-6	0.162	-0.120	-0.002	0.167	-0.094	0.006	0.165	-0.186	-0.018	0.166	-0.176	-0.014
-5	0.147	-0.091	-0.001	0.153	-0.071	0.006	0.148	-0.153	-0.014	0.149	-0.147	-0.011
-4	0.135	-0.074	0.000	0.139	-0.053	0.005	0.134	-0.126	-0.011	0.135	-0.120	-0.009
-3	0.122	-0.059	0.001	0.128	-0.043	0.005	0.122	-0.102	-0.008	0.123	-0.098	-0.007
-2	0.112	-0.047	0.003	0.116	-0.041	0.004	0.113	-0.083	-0.004	0.113	-0.082	-0.004
-1	0.106	-0.041	0.005	0.110	-0.043	0.005	0.107	-0.070	0.000	0.106	-0.071	0.000
0	0.104	-0.040	0.008	0.106	-0.046	0.007	0.104	-0.061	0.004	0.103	-0.063	0.004
+1	0.105	-0.039	0.010	0.107	-0.047	0.009	0.105	-0.054	0.007	0.104	-0.056	0.007
+2	0.110	-0.036	0.013	0.110	-0.044	0.012	0.110	-0.045	0.009	0.110	-0.049	0.009
+3	0.115	-0.030	0.016	0.115	-0.038	0.015	0.119	-0.037	0.011	0.117	-0.042	0.011
+4	0.127	-0.016	0.019	0.126	-0.024	0.018	0.129	-0.029	0.013	0.128	-0.034	0.012
+5	0.142	-0.002	0.020	0.141	-0.011	0.019	0.142	-0.020	0.013	0.141	-0.025	0.012
+6	0.159	0.009	0.020	0.158	-0.003	0.019	0.156	-0.008	0.014	0.157	-0.014	0.013
+7	0.176	0.024	0.023	0.174	0.010	0.021	0.174	0.005	0.015	0.172	-0.004	0.013
+8	0.190	0.049	0.028	0.188	0.031	0.025	0.189	0.017	0.015	0.189	0.006	0.014
+9	0.203	0.071	0.033	0.202	0.056	0.030	0.206	0.031	0.017	0.206	0.022	0.015
+10	0.217	0.094	0.038	0.216	0.080	0.035	0.222	0.046	0.019	0.222	0.037	0.017

Table 6.1. The static force coefficients with angle of incidence.

7. Indicative Vortex-Shedding Tests

In extension to providing static load coefficients, the section model set-up in the static rig was also used to investigate dynamic wind loads on the bridge section. When performed in smooth flow such measurements are particularly useful in determining the harmonic loading caused by vortex shedding around the bridge deck. As the static rig is in reality a dynamic rig with very high stiffness and relatively low damping, lock-in may be encountered resulting in larger dynamic forces. The magnitude of these dynamic forces is an indication of the susceptibility of the bridge deck to vortex-shedding induced vibration and is mainly intended for comparison between different sections.

In the present case, potential vortex-induced vibrations of the deck was investigated in smooth flow in the static rig in this indicative manner. The wind speed was gradually increased and the dynamic vertical response is observed in terms of mapping the lift force and measuring the vertical acceleration at mid span on the model. The acceleration was double integrated to obtain the rms displacement at mid span.

Testing was performed at 0° angle of attack and with the model inherent damping (approximately 0.4% of critical).

The response in terms of vertical rms response was mapped out as function of wind speed.

The bending frequency of the model was approximately 9.6Hz. The 2.55m long model weighed 9.8kg in the present in-service condition.

The Scruton number is typically defined as: $Sc = (\delta \cdot \mu)/(\rho \cdot B^2)$, where δ is the damping as logarithmic decrement ($\approx 2\pi \cdot 0.4\% = 2.5\%$ in the present case), μ is the mass per unit length of the model (½·9.8kg / 2.55m =1.92kg/m, where the factor ½ accounts for the sinusoidal mode-shape of the model when mounted in the static rig), ρ is the air density (approximately 1.2kg/m^3) and B is the deck width (60.4m/80=0.755m). With this definition and these values, the Scruton number in the tests is expected to be around $Sc \approx 0.07$.

The results of the tests are presented in Figure 7.1.

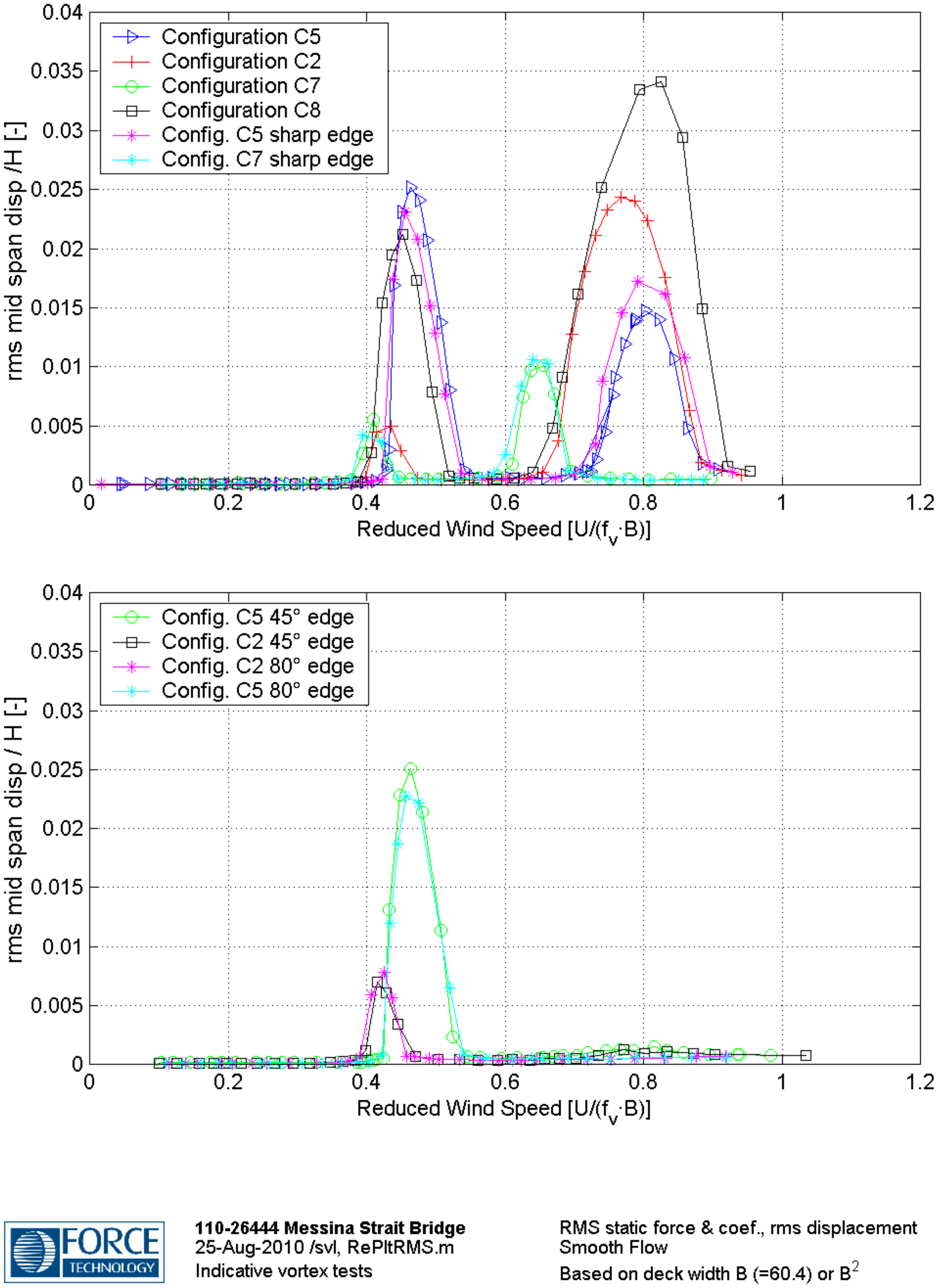

Figure 7.1. Results of indicative vortex-shedding tests.

8. Stability & Damping Tests

The test set-up and methods were identical to those in the previous tests, see [4]. Due to the time constraints in the test execution, a full mass calibration of the rig was not performed. However, the present model - with the same ballast as in the previous tests - resulted in frequencies within two percent of the target values. Thus, the mass and mass moment of inertia were matched within approximately 4%.

The obtained frequencies and estimated mass properties are compared with the target values in the table below.

The resulting velocity scaling for the vertical and torsional response in the dynamic rig (Soft Rig) was approximately 1:6.4, 1 m/s in the wind tunnel corresponding to 6.4 m/s in full-scale.

	Prototype		**Section Model Soft Rig**	
	"Vacuum"	"In-Air"	Target	Obtained
$f_{vertical}$ (Hz)	0.0645	0.064	0.797	0.81
$f_{torsional}$ (Hz)	0.0831	0.083	1.031	1.02
Ratio: $f_{torsional}$ / $f_{vertical}$	1.29	1.29	1.29	1.26
Mass per unit length (kg/m)	53,200	53,683	8.388	8.24*
Mass moment of inertia per unit length (kg·m^2/m)	26,500,000	26,650,092	0.651	0.62*

Table 8.1. Dynamic properties of prototype structure and section model.
*Estimated values.

The model was restrained in the lateral direction, the horizontal motions of the deck having no significant influence on the stability of the deck, which is the normal assumption for section model tests.

In the dynamic rig (soft rig) the damping for vertical motion was approximately 0.3% of critical and for torsional motion it was about 0.2% of critical.

8.1 Stability Tests

The dynamic section model tests aimed at defining the aerodynamic stability limit of the deck. In the current tests, the stability limit of configuration C2 with 45° rail girder edge was investigated in smooth and turbulent flow for angles of wind incidence of -4°, 0° and +4°. In addition, C5 with 45° rail girder edge was studied in smooth flow at +4°.

Variations of the mean and root-mean-square (rms) responses with reduced mean wind speeds at deck level are presented in the form of mean and rms vertical displacement normalised by the deck height (4.68 m full-scale). The pitch response is simply presented as the deck rotation in degrees. This section presents summary plots of the results obtained in the dynamic section model tests.

A summary of the main findings is given in Section 2. The detailed presentation given in Appendix A includes plots of the peak factor. The definition of the peak factor is given overleaf.

$$peak\ \ factor = \frac{d_{\max} - d_{\min}}{2 \cdot rms} \tag{7.2}$$

d_{max} and d_{min} are the maximum and minimum values (e.g., deflection) of a given time series, respectively, and rms is the root-mean-square of the time series.

Each of the data points (except from the last point, where instability starts) on the response plots results from the measurements of stable, limited amplitude motion (as opposed to a negative total damping case where the amplitude continues to grow in magnitude for the same wind speed). The peak factor can be used to see whether the motion is in a "locked-in" state of sinusoidal motion or a random type motion.

The onset of an "instability" is defined as when the character of the response changes from a random type motion to that of a regular, sinusoidal motion, involving either pure torsional, pure vertical or a coupled vertical-torsional vibration. This can often be identified through an examination of the peak factor. A random signal has peak factors in the 3-4 range, while a pure sinusoid has a peak factor of √2 or 1.41. Alternatively, a torsional rms response of 0.5° can be chosen as the governing criteria.

However, in the present tests the identification of instability has been difficult in some cases due to the large buffeting response. It was not possible to obtain time series of the response where the harmonic response of starting instability could be observed in the peak factors. Consequently the test speed was gradually increased (and the response measured) until the self excited motion was observed or the test had to be stopped due to large response in order to safeguard the model and the rig.

Figure 8.1 shows results from the stability tests in terms of rms response.

*For the configuration C2 / 45° in smooth flow at +4°, a limit-cycle response (i.e., large response self-limited in amplitude) was observed for this configuration and angle of attack for wind speeds lower than the estimated critical wind speed. The amplitudes were so large that the peak of the response curve could not be measured. Consequently, the wind speed was increased beyond the wind speed range the with limit-cycle motion.

The limit-cycle responses were dominated by vertical motion and with a moderate torsional response, the latter with a frequency coinciding with the vertical frequency.

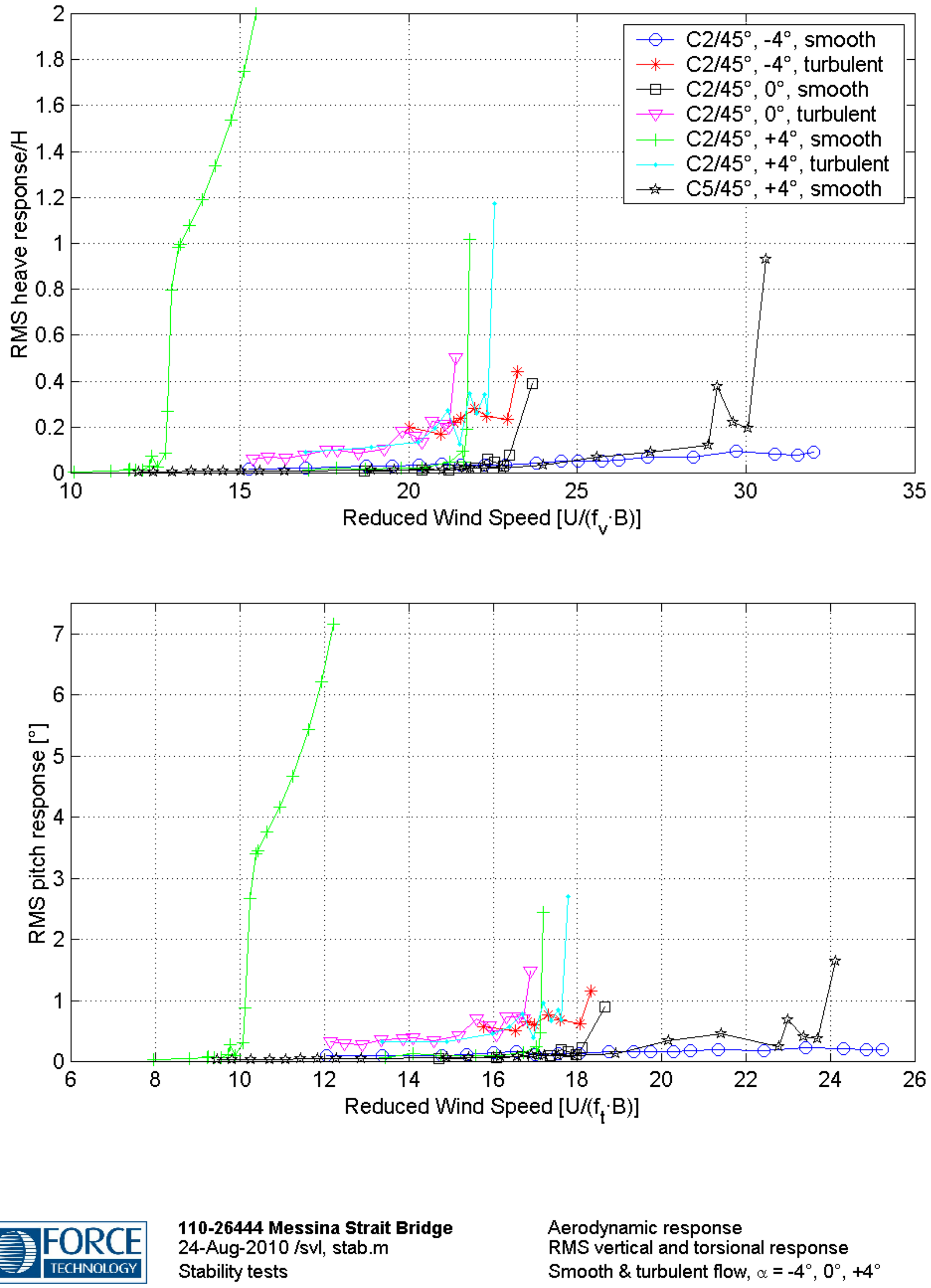

Figure 8.1. Response in stability tests.

8.2 Damping Tests

The damping level (i.e., the sum of the aerodynamic and structural damping) has been estimated in connection with the stability tests. At wind speeds corresponding to 54 m/s and 75 m/s (full-scale), respectively, the model was given a combined displacement in torsional and vertical direction (pitch and heave). Subsequently the model was released and the decay signals were recorded. Based on the decay signals the damping levels have been estimated. It should be noted that in some cases - especially at the higher wind speed – the damping was high and therefore for these cases the damping has been estimated based on a limited number of cycles of motion and consequently the damping estimation is a rough approximation. In many cases, the obtained decay signals exhibited damping level that was strongly amplitude dependent.

The vertical damping is presented for amplitudes up to 20 – 40 mm and the torsional damping is presented for an amplitude of approximately 1° - 2°.

The tests results are summarized in the following table. In this table "C2/45°" refers to *C2 45° rail girder edge.* The negative damping for C2/45° at 54 m/s is due to the limit-cycle motion described in Section 8.1.

Configuration	U [m/s]	flow	angle [°]	vertical damping [% crit]	torsional damping [% crit]
C2/45°	54	Turbulent	0	5.5	2.0
C2/45°	75	Turbulent	0	0.6	0.6
C2/45°	54	Smooth	0	2.1	1.3
C2/45°	75	Smooth	0	2.7	1.9
C2/45°	54	Smooth	-4	2.3	2
C2/45°	75	Smooth	-4	1.8	2.1
C2/45°	54	Turbulent	-4	3.1	1.9
C2/45°	75	Turbulent	-4	0.9	1.2
C2/45°	54	Turbulent	+4	3.1	1.5
C2/45°	75	Turbulent	+4	1.0	1.5
C2/45°	54	Smooth	+4	-1.2	-1.1
C2/45°	75	Smooth	+4	4.5	3.2

Table 8.2 Estimated damping levels (in % of critical).

9. References

[1] "Section Model Tests for the Messina Strait Crossing, Italy"
FORCE 2005011 rev. 3.1, 2005-04-18

[2] "Stability Tests for Modified Deck for the Messina Strait Crossing, Italy"
FORCE 2005263 rev. A, 2005-12-22

[3] "Static section model tests the Messina Strait Bridge"
FORCE 109-28238 rev. 1, 2010-01-13

[4] "Sub-Test 1 Section Model Tests for the Messina Strait Bridge"
FORCE 110-25465 rev. 1, 2010-06-25

APPENDIX A

Stability Tests – Response Plots

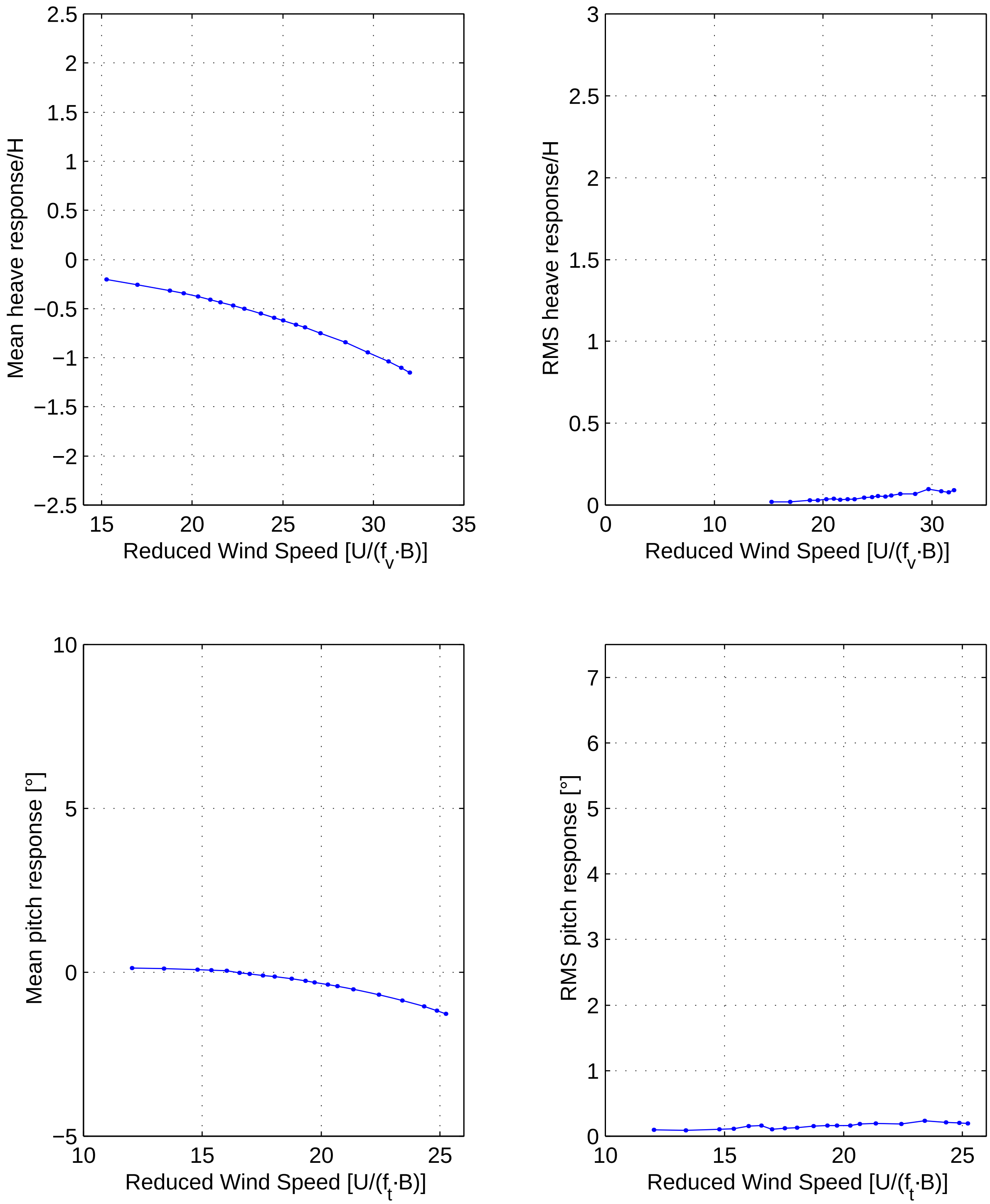

110−26444 Messina Strait Bridge
25−Aug−2010 /svl, stab.m
Mean and RMS Response

Stability Tests
Configuration C2 − 45° railway girder edge
Smooth flow, $\alpha = -4^{o}$

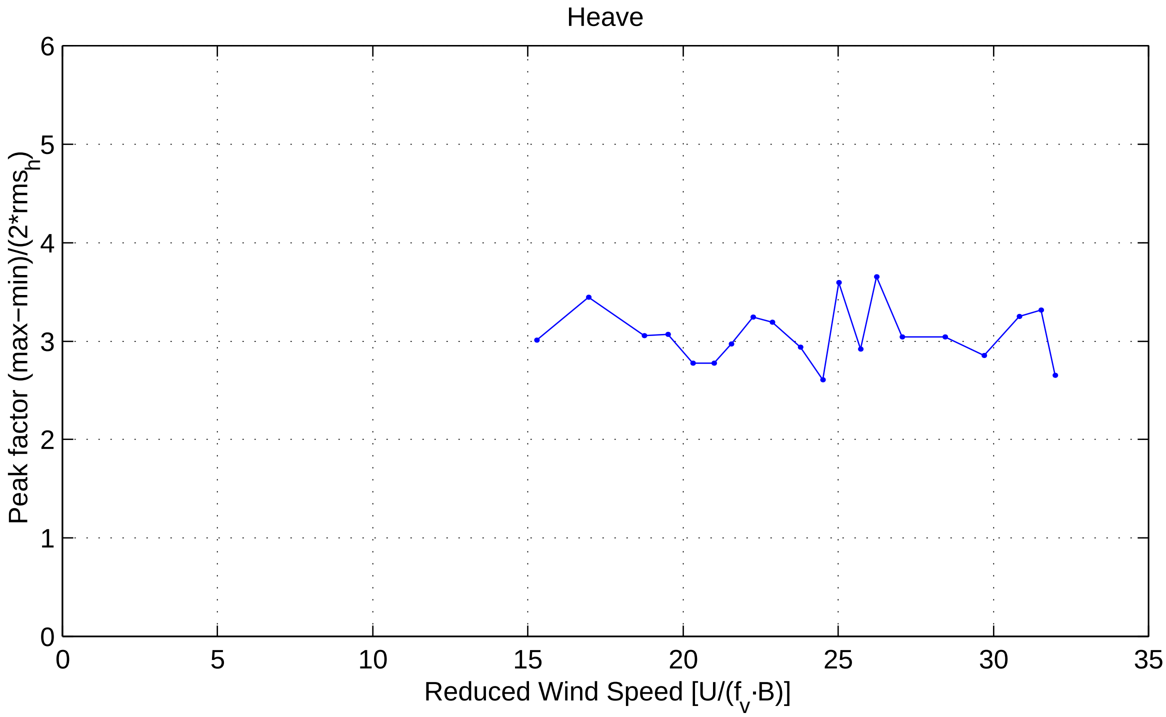

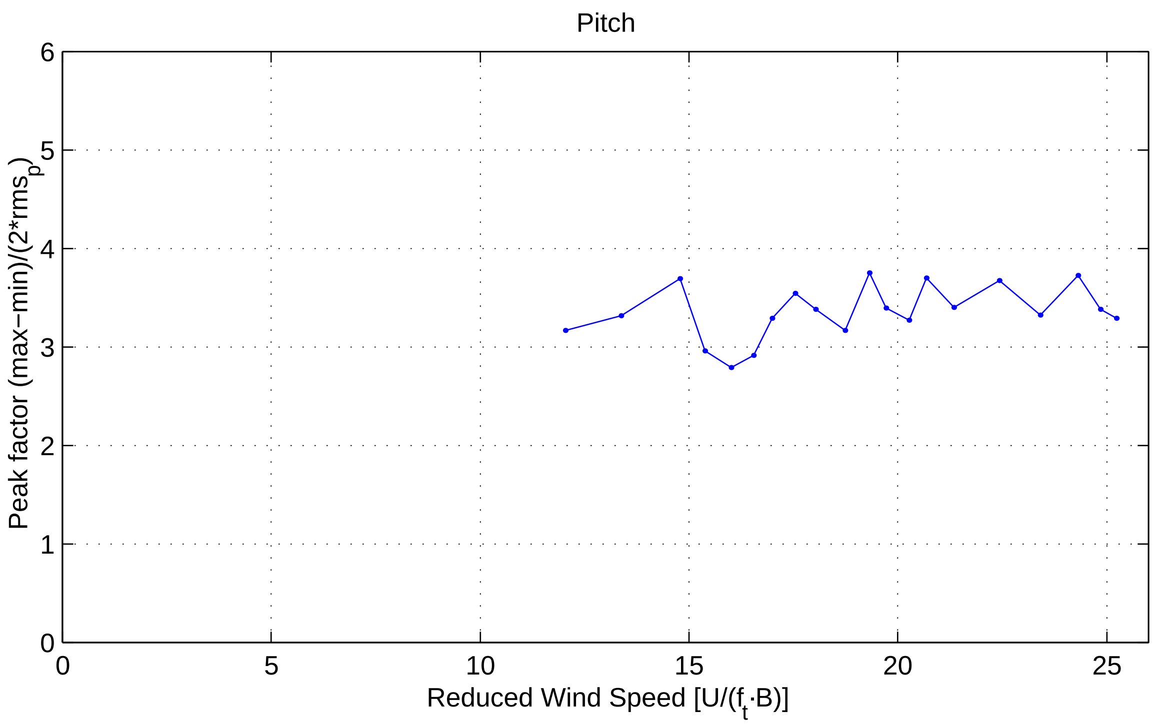

110−26444 Messina Strait Bridge
25−Aug−2010 /svl, stab.m
Peak factors

Stability Tests
Configuration C2 − 45° railway girder edge
Smooth flow, $\alpha = -4^o$

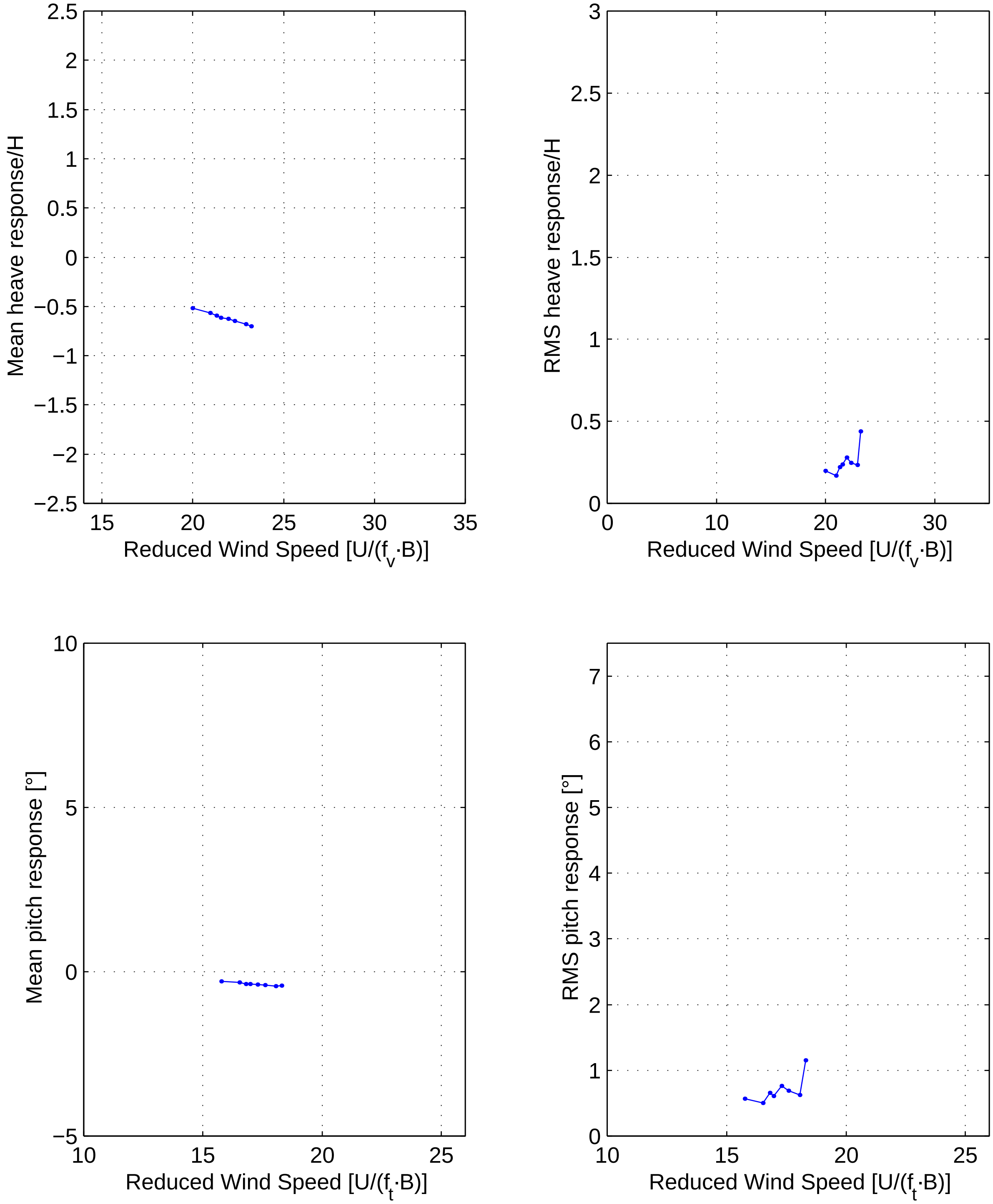
Mean heave response/H
Reduced Wind Speed [U/(f_v·B)]
RMS heave response/H
Reduced Wind Speed [U/(f_v·B)]
Mean pitch response [°]
Reduced Wind Speed [U/(f_t·B)]
RMS pitch response [°]
Reduced Wind Speed [U/(f_t·B)]

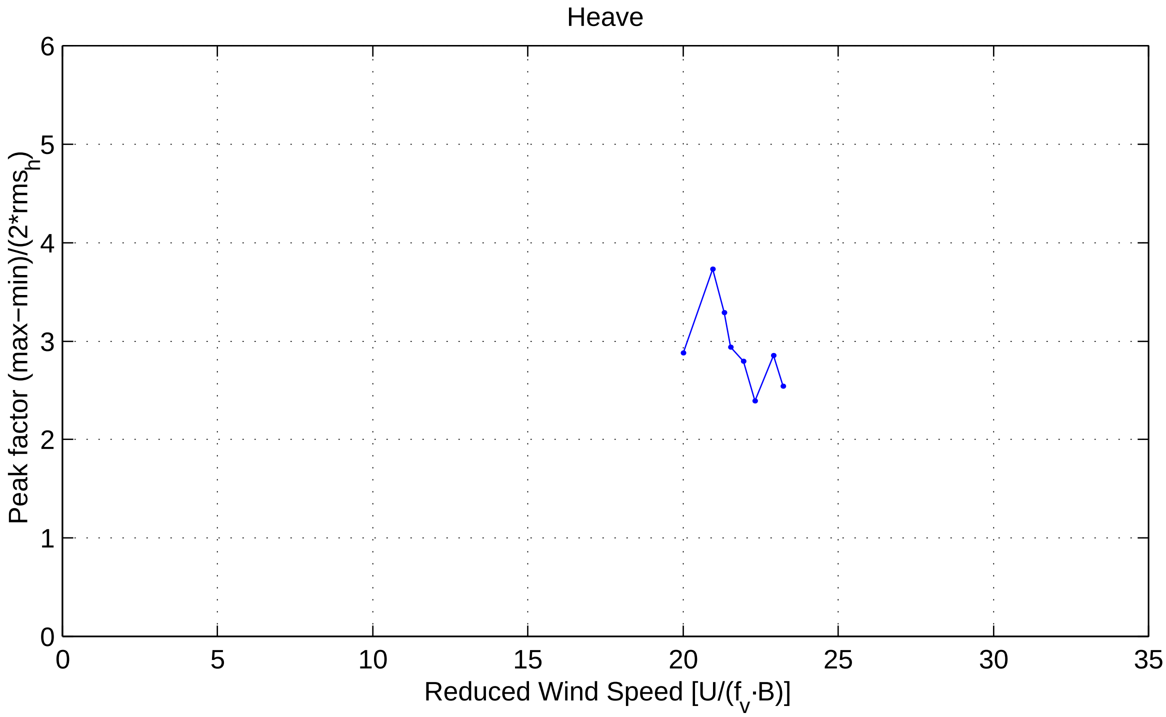
Heave
Peak factor (max−min)/(2*rms_h)
Reduced Wind Speed [U/(f_v·B)]

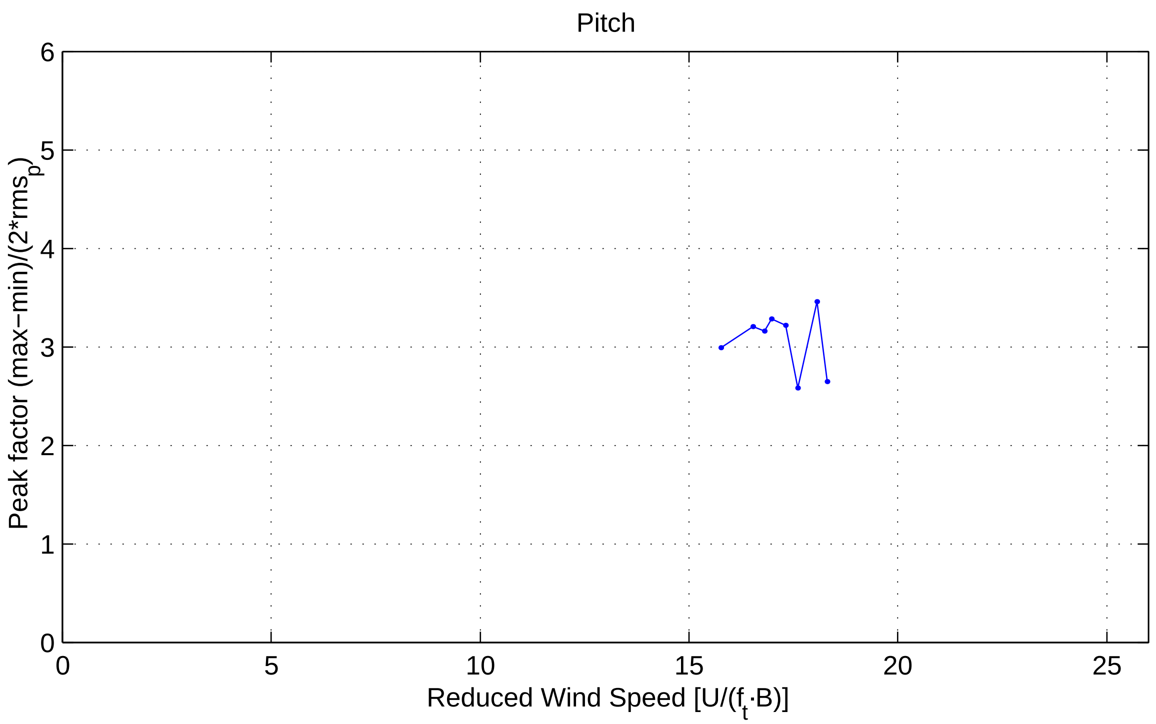
Pitch
Peak factor (max−min)/(2*rms_p)
Reduced Wind Speed [U/(f_t·B)]

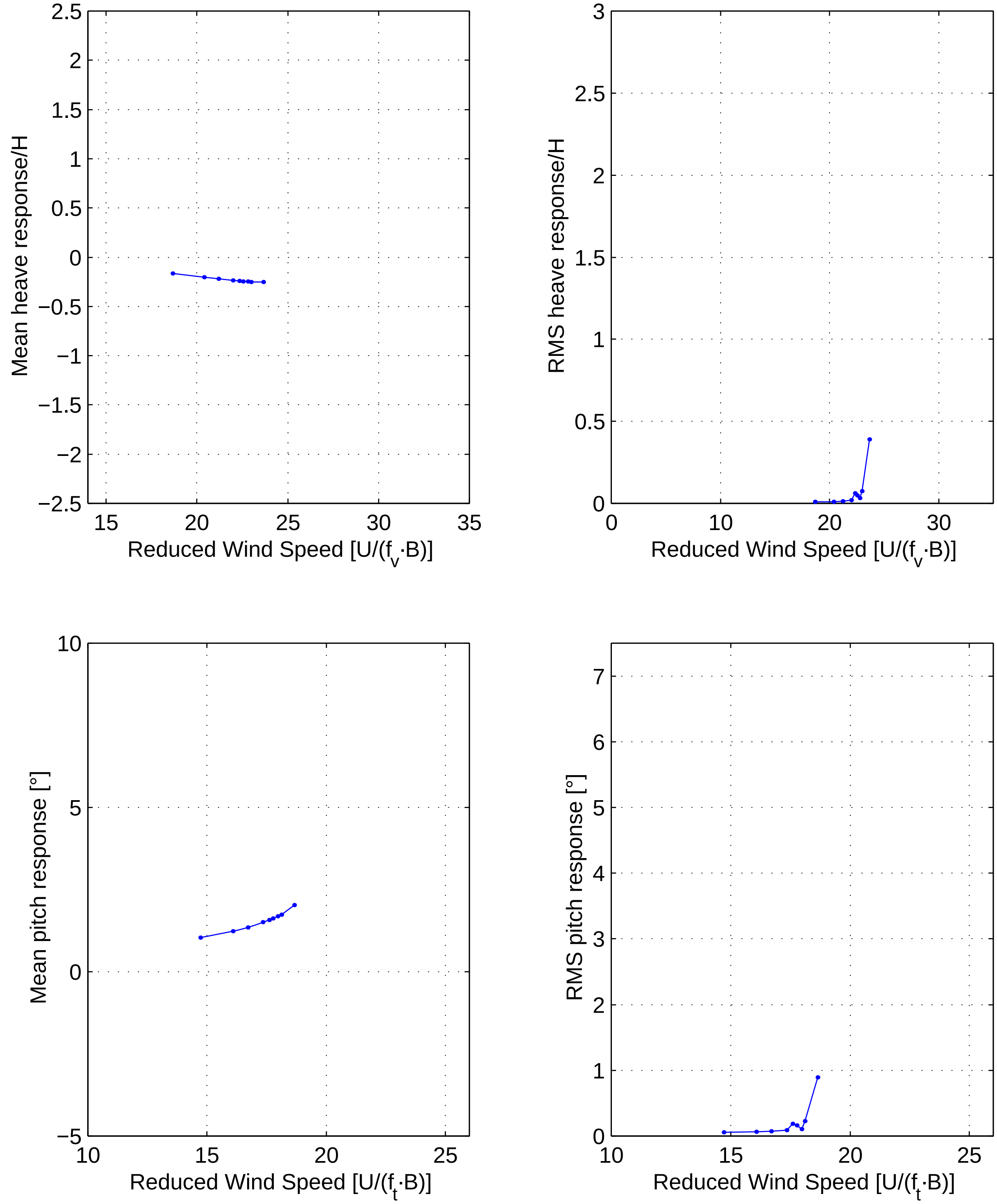

Mean heave response/H
Reduced Wind Speed [U/(f_v·B)]
RMS heave response/H
Reduced Wind Speed [U/(f_v·B)]
Mean pitch response [°]
Reduced Wind Speed [U/(f_t·B)]
RMS pitch response [°]
Reduced Wind Speed [U/(f_t·B)]

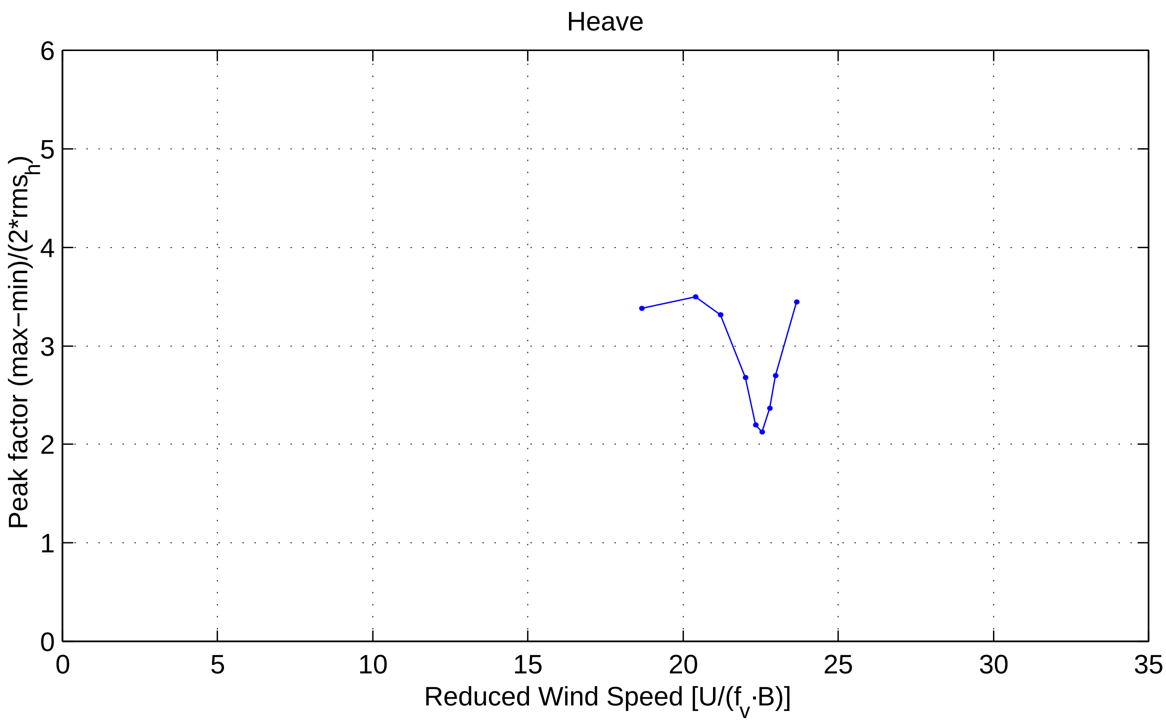
Heave
Peak factor (max−min)/(2*rms_h)
Reduced Wind Speed [U/(f_v·B)]
0
1
2
3
4
5
6
0
5
10
15
20
25
30
35

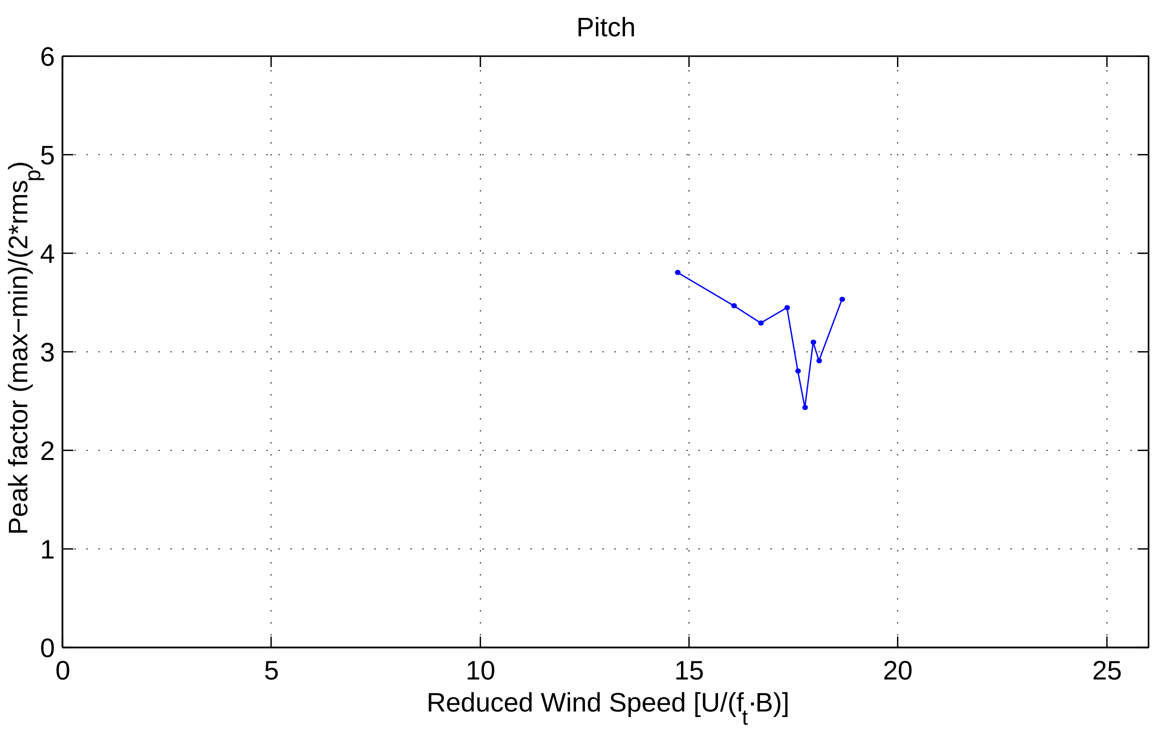
Pitch
Peak factor (max−min)/(2*rms_p)
Reduced Wind Speed [U/(f_t·B)]
0
1
2
3
4
5
6
0
5
10
15
20
25

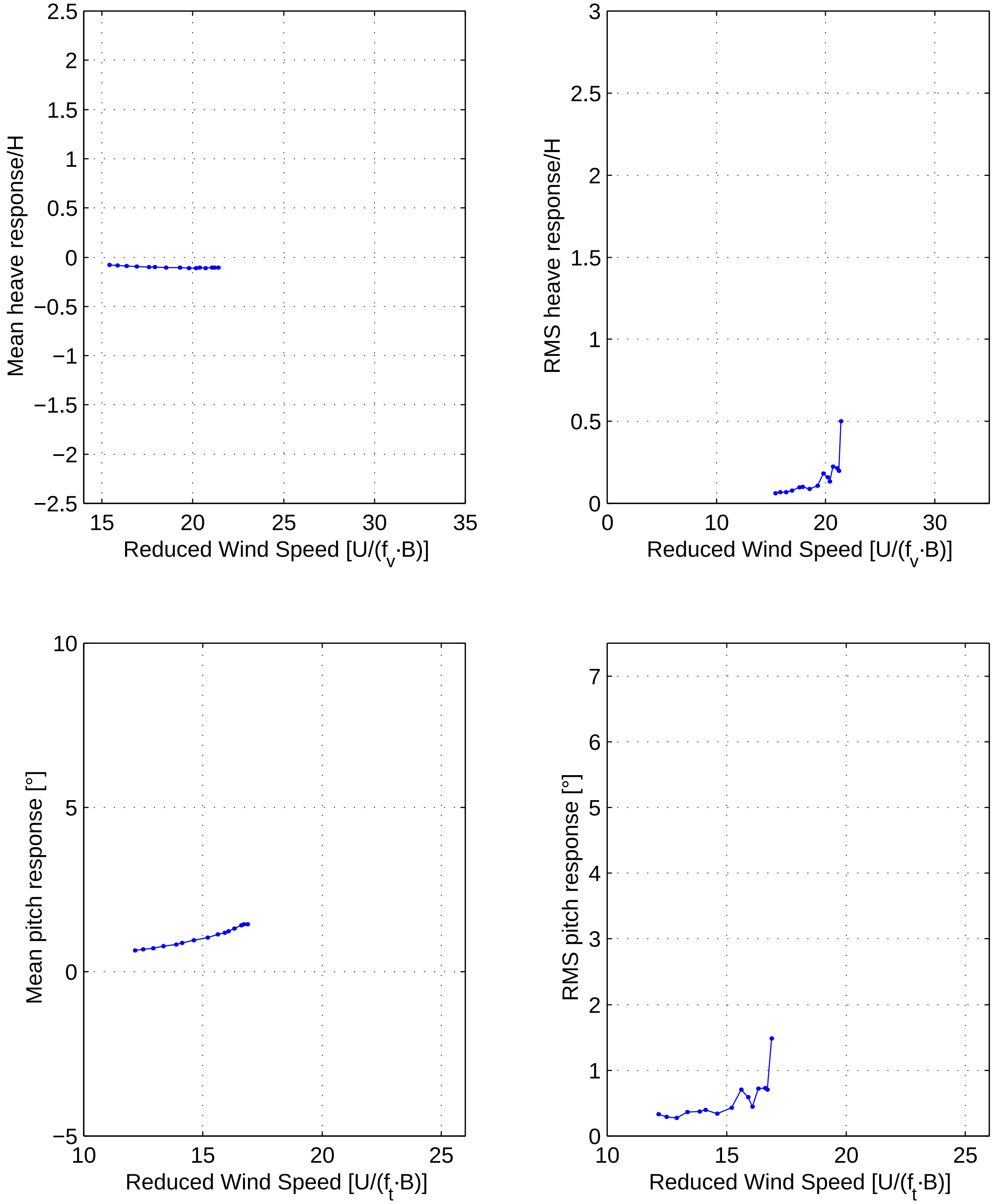
Mean heave response/H
Reduced Wind Speed [U/(f_v·B)]
RMS heave response/H
Reduced Wind Speed [U/(f_v·B)]
Mean pitch response [°]
Reduced Wind Speed [U/(f_t·B)]
RMS pitch response [°]
Reduced Wind Speed [U/(f_t·B)]

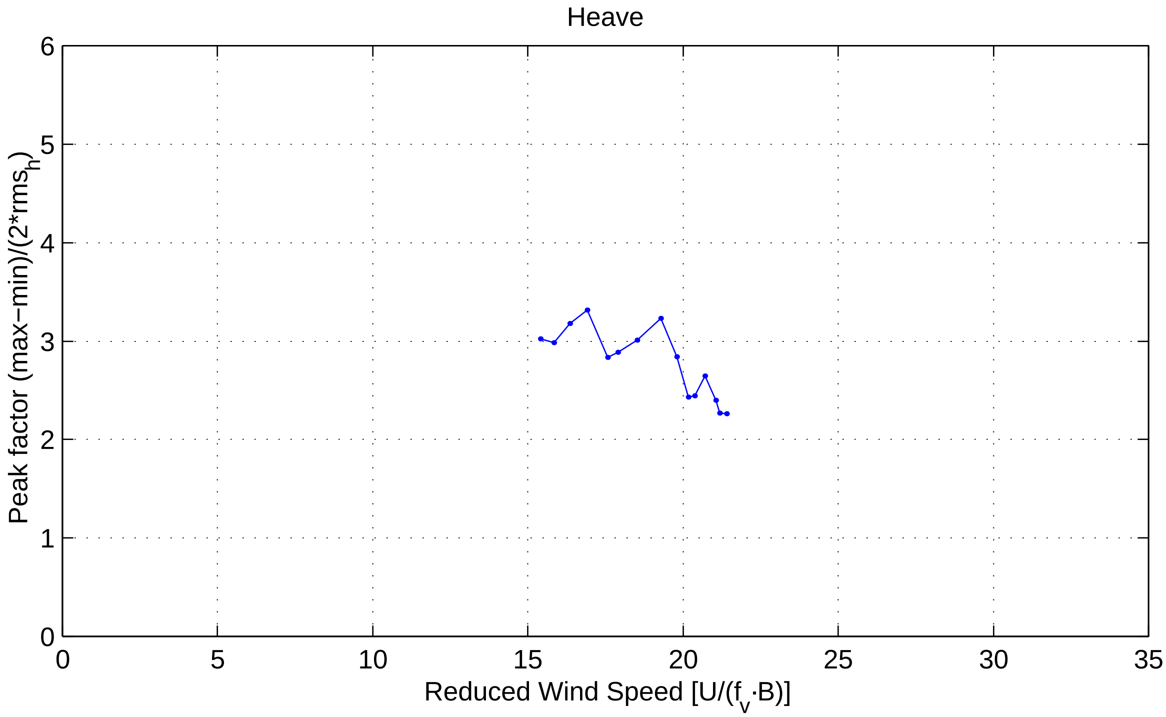

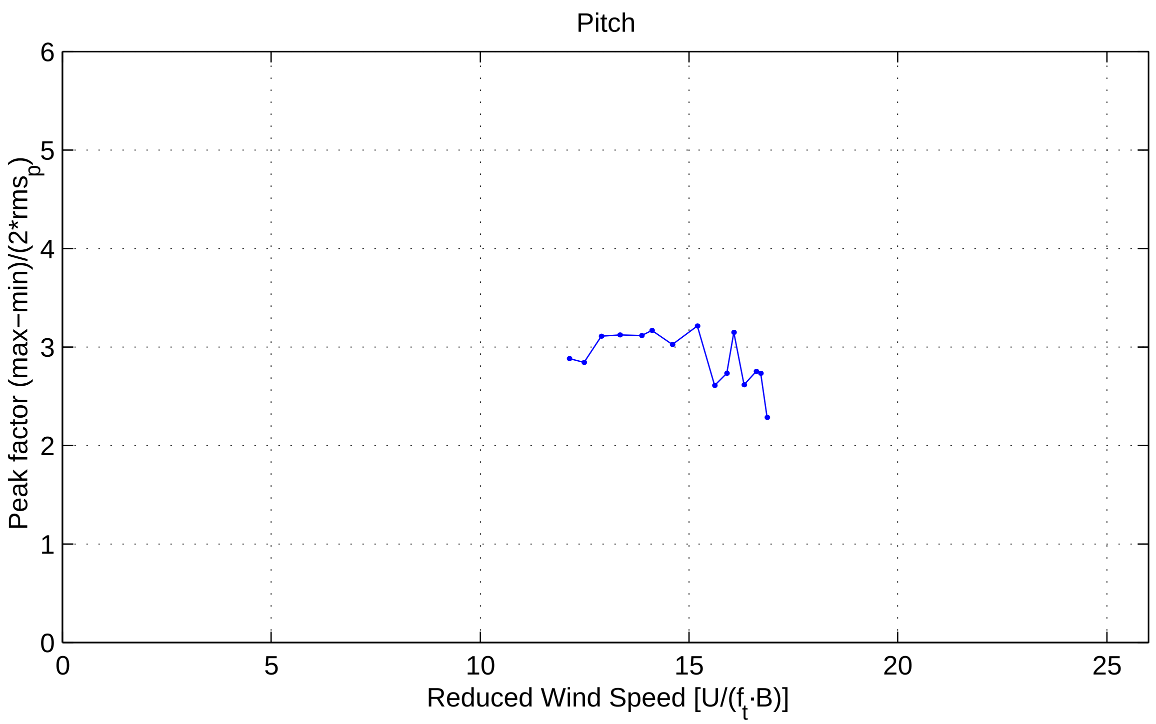

110−26444 Messina Strait Bridge
25−Aug−2010 /svl, stab.m
Peak factors

Stability Tests
Configuration C2 − 45° railway girder edge
Turbulent flow, α = 0º

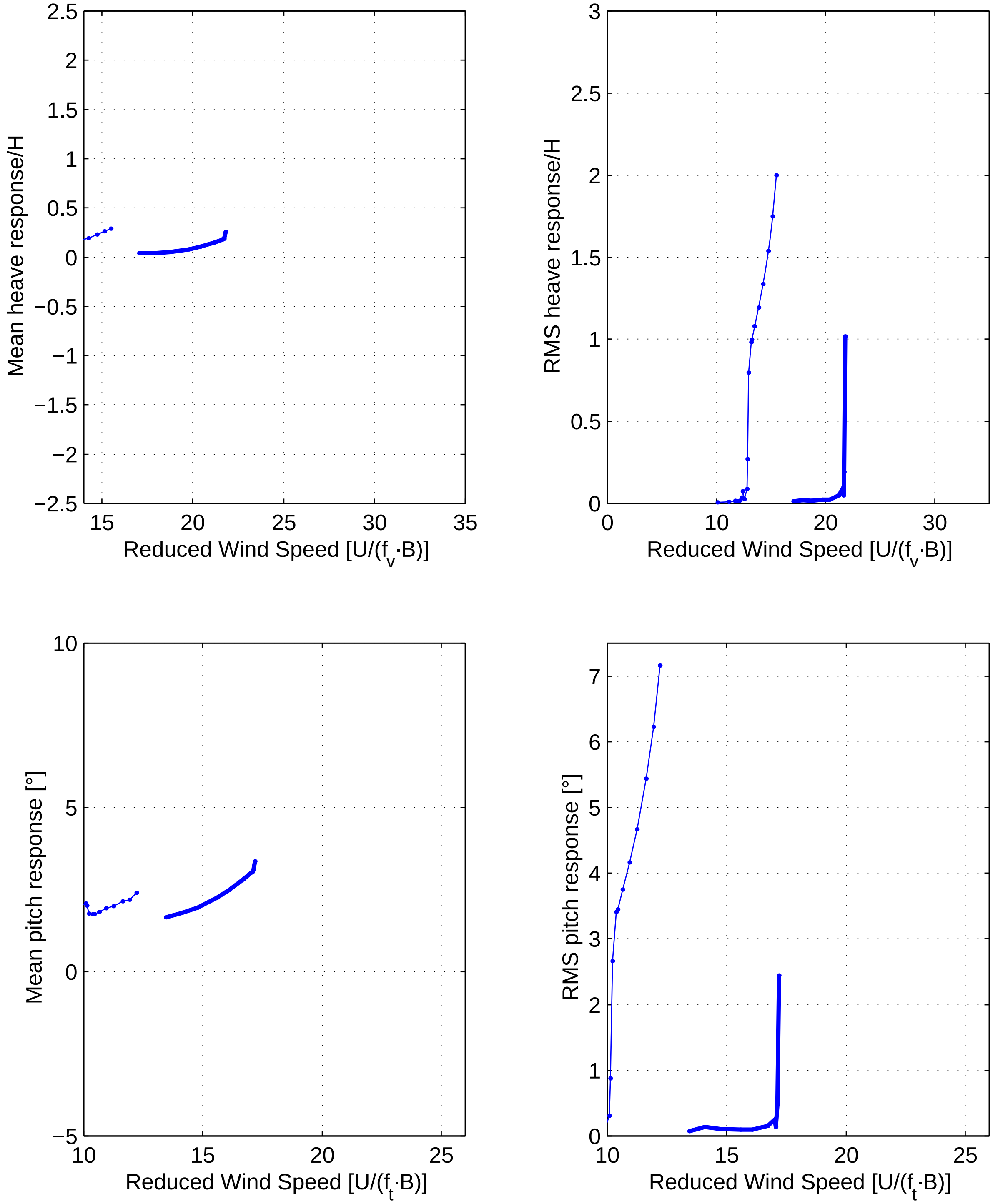

110−26444 Messina Strait Bridge
25−Aug−2010 /svl, stab.m
Mean and RMS Response

Stability Tests
Configuration C2 − 45° railway girder edge
Smooth flow, α = +4º

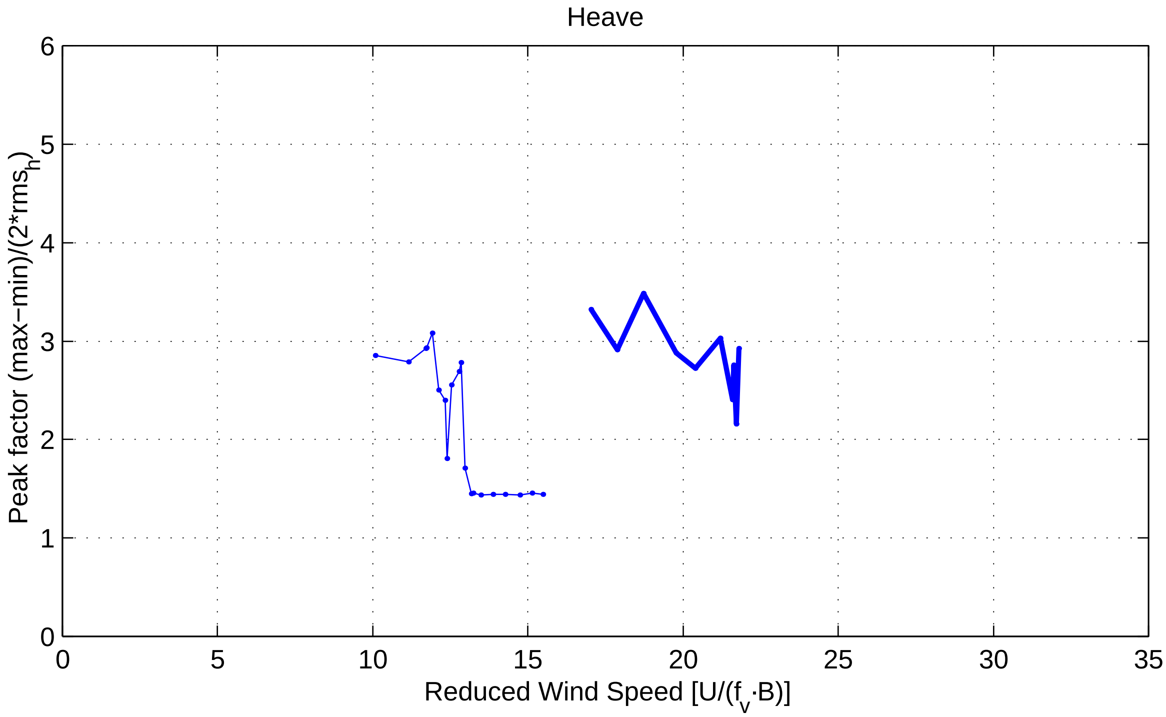
Heave
Peak factor (max−min)/(2*rms$_h$)
Reduced Wind Speed [U/(f$_v$·B)]
0
1
2
3
4
5
6
0
5
10
15
20
25
30
35

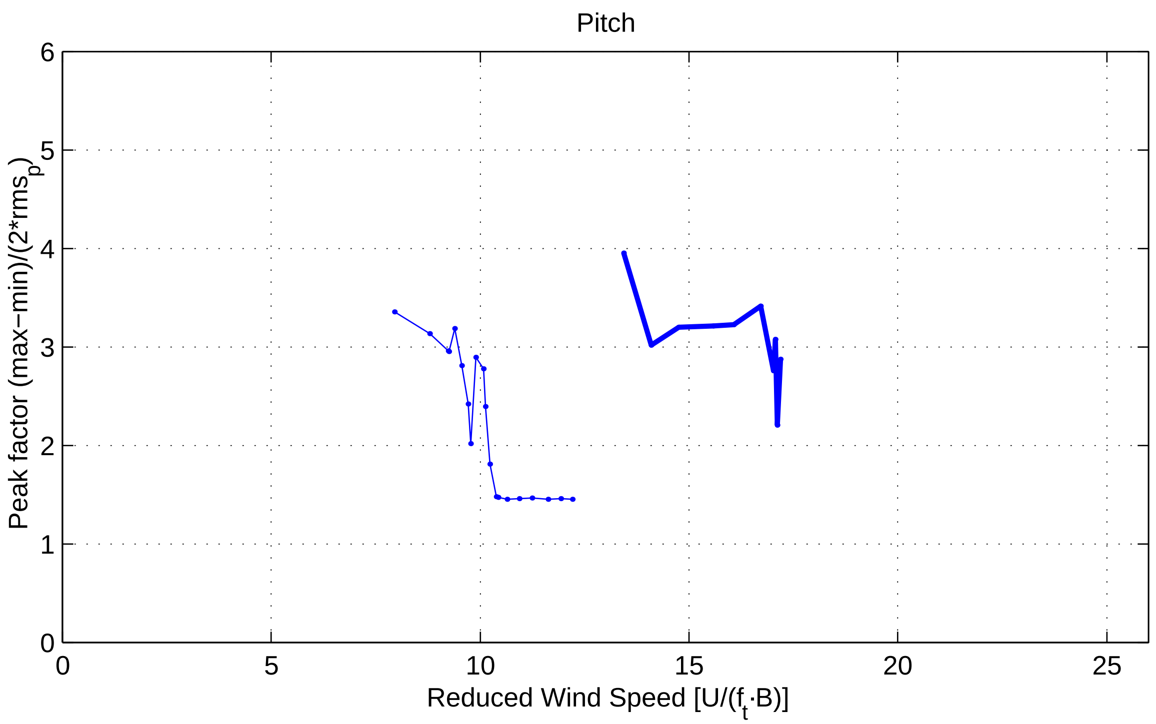
Pitch
Peak factor (max−min)/(2*rms$_p$)
Reduced Wind Speed [U/(f$_t$·B)]
0
1
2
3
4
5
6
0
5
10
15
20
25

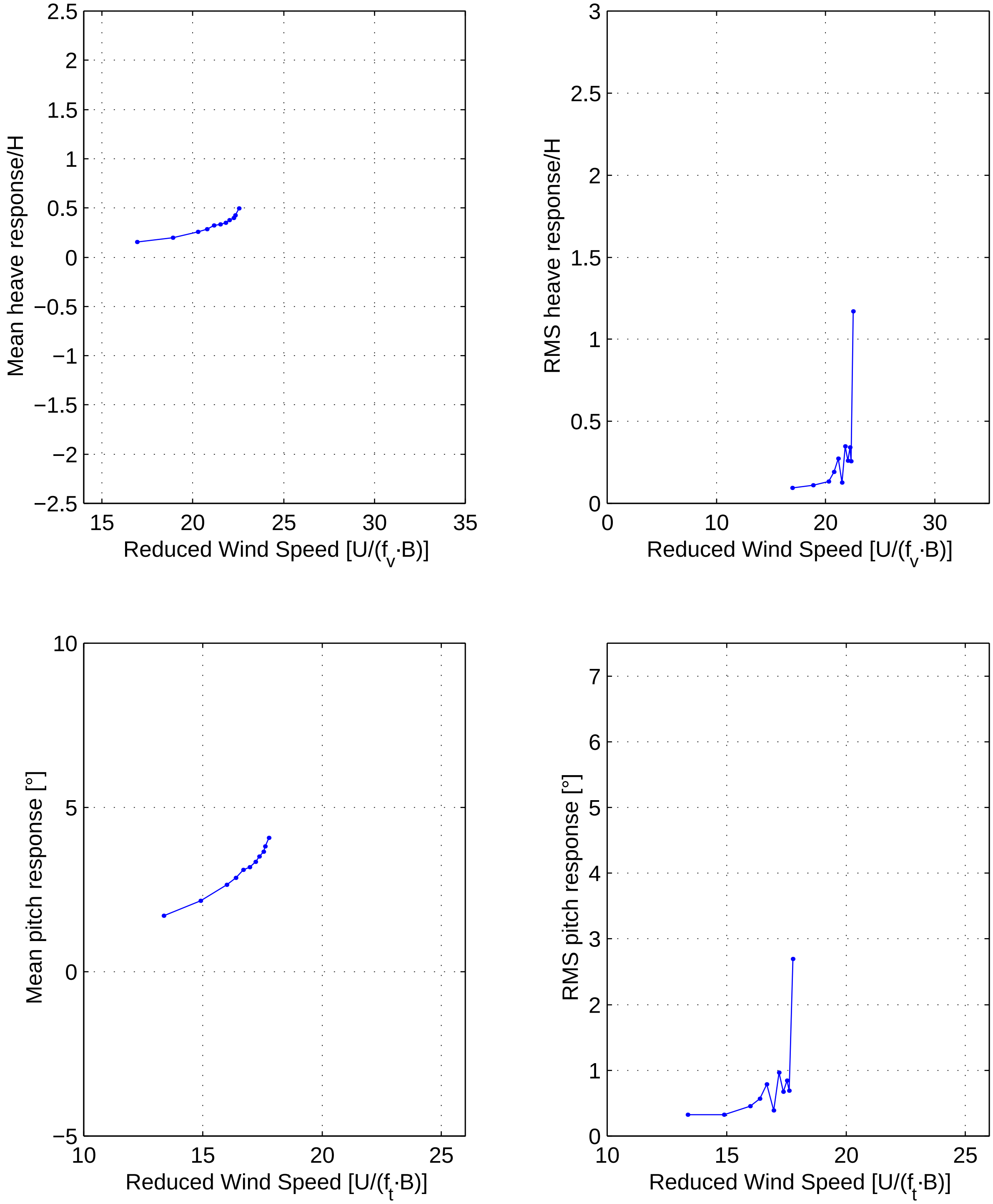

110−26444 Messina Strait Bridge
25−Aug−2010 /svl, stab.m
Mean and RMS Response

Stability Tests
Configuration C2 − 45° railway girder edge
Turbulent flow, α = +4º

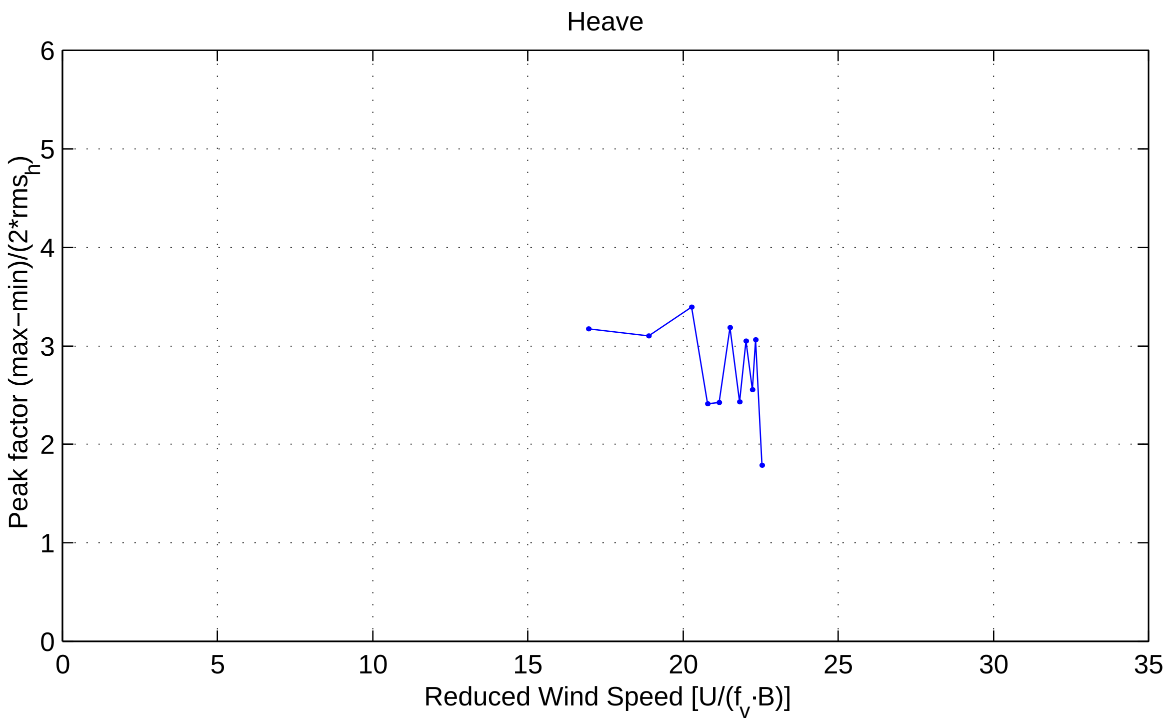

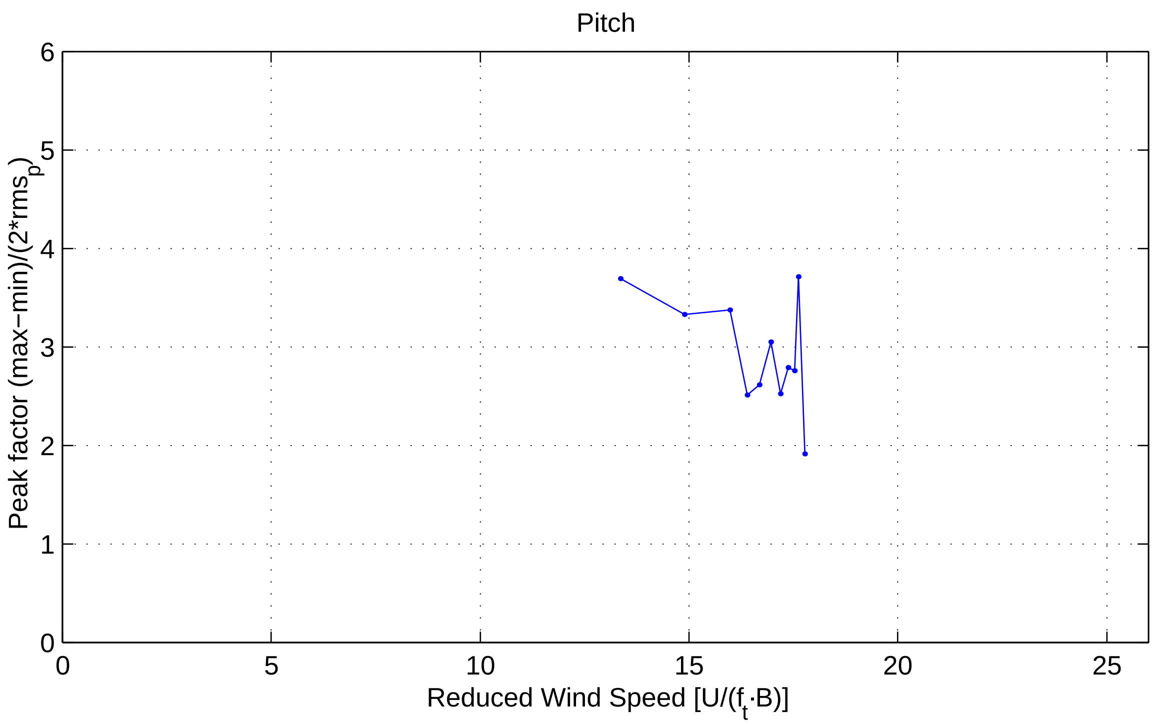

FORCE TECHNOLOGY

110−26444 Messina Strait Bridge
25−Aug−2010 /svl, stab.m
Peak factors

Stability Tests
Configuration C2 − 45° railway girder edge
Turbulent flow, $\alpha = +4^{o}$

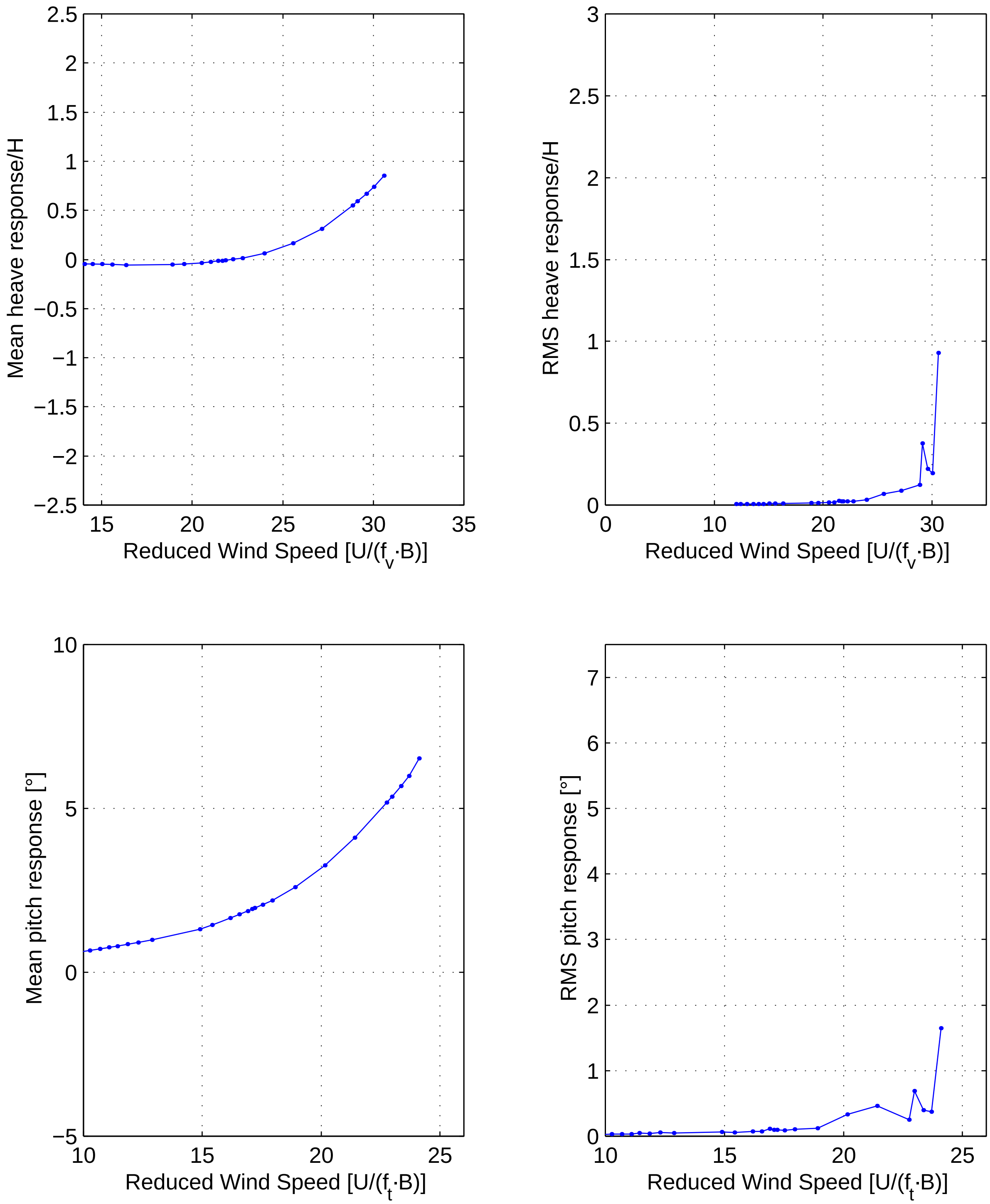

FORCE TECHNOLOGY

110−26444 Messina Strait Bridge
25−Aug−2010 /svl, stab.m
Mean and RMS Response

Stability Tests
Configuration C5 − 45° railway girder edge
Smooth flow, α = +4º

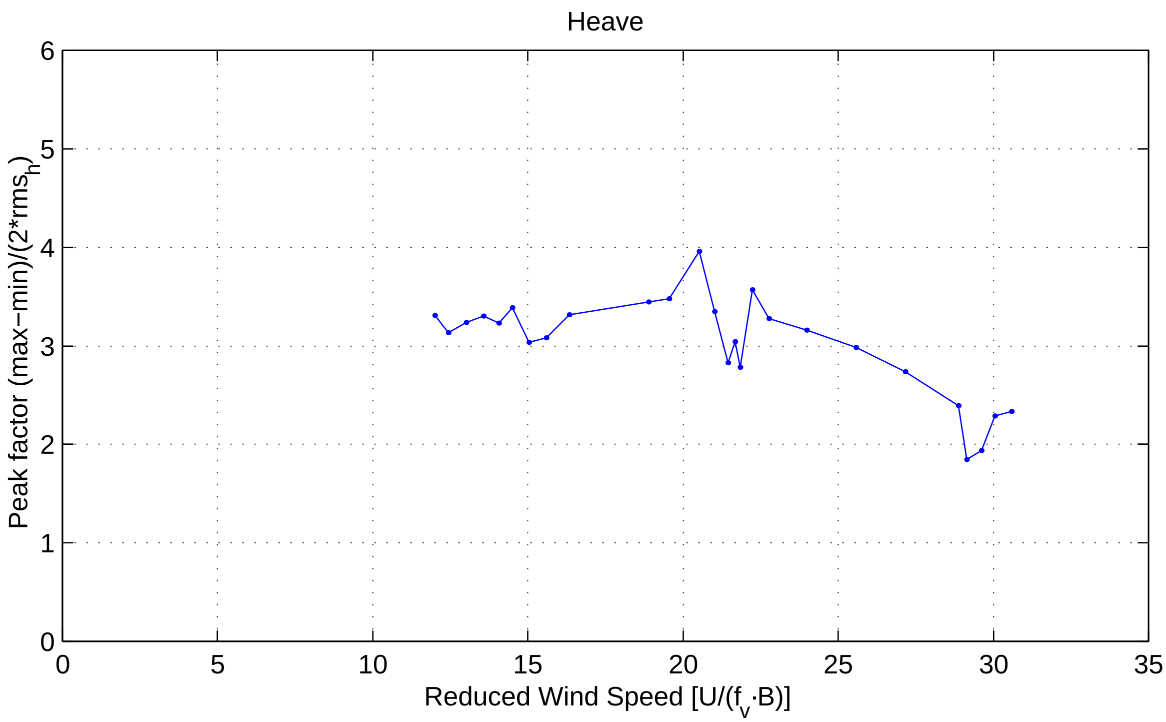
Heave
Peak factor (max−min)/(2*rms_h)
Reduced Wind Speed [U/(f_v·B)]
0
5
10
15
20
25
30
35
0
1
2
3
4
5
6

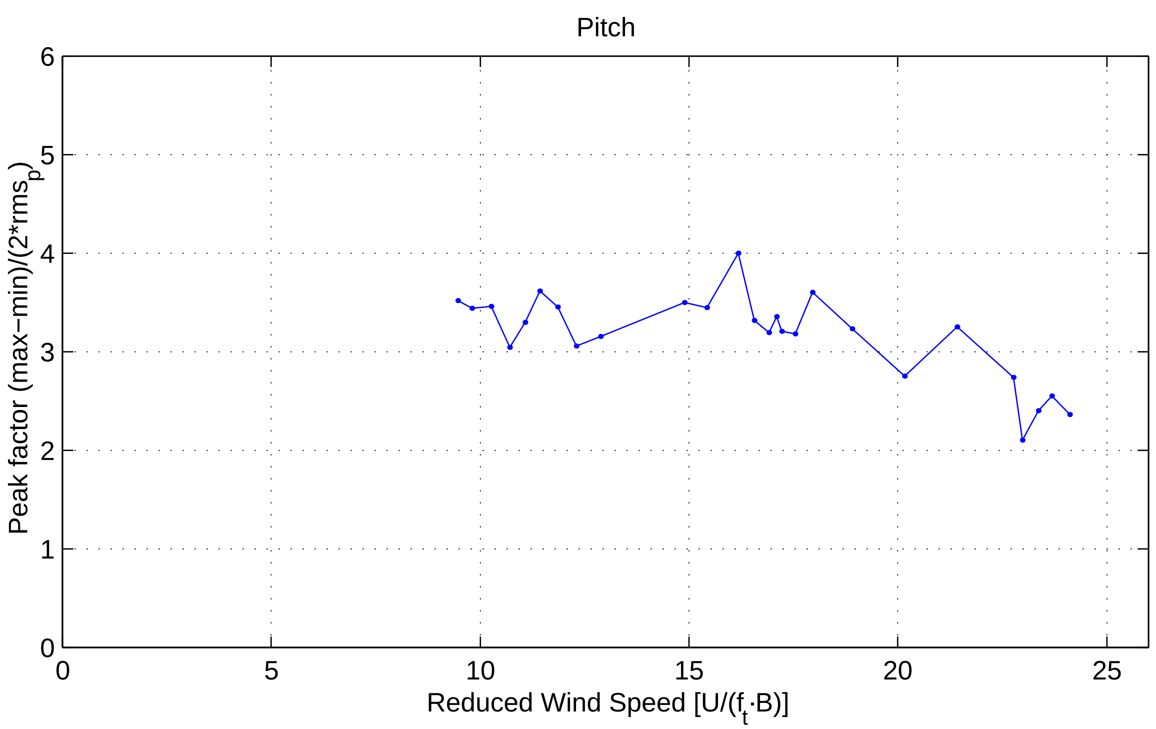
Pitch
Peak factor (max−min)/(2*rms_p)
Reduced Wind Speed [U/(f_t·B)]
0
5
10
15
20
25
0
1
2
3
4
5
6

FORCE Technology
Division for Maritime Industry
Hjortekærsvej 99
2800 Kgs. Lyngby, Denmark
Tel. +45 72 15 77 00
Fax +45 72 15 77 01
force@force.dk
www.force.dk

FORCE Technology
Headquarters
Park Allé 345
2605 Brøndby, Denmark
Tel. +45 43 26 70 00
Fax +45 43 26 70 11
force@force.dk
www.force.dk